Collisional-radiative nonequilibrium in partially ionized atomic nitrogen

J. A. Kunc and W. H. Soon
Department of Aerospace Engineering and Department of Physics, University of Southern California, Los Angeles, California 90089-1191
(Received 13 January 1989)

A nonlinear collisional-radiative model for determination of nonequilibrium production of electrons, excited atoms, and bound-bound, dielectronic and continuum line intensities in stationary partially ionized atomic nitrogen is presented. Populations of 14 atomic levels and line intensities are calculated in plasma with $8000 \leq T_e \leq 15\,000$ K and $10^{12} \leq N_t \leq 10^{18}$ cm^{-3}. Transport of radiation is included by coupling the rate equations for production of the electrons and excited atoms with the radiation escape factors, which are not constant but depend on plasma conditions.

I. INTRODUCTION

The objective of this work is to formulate a collisional-radiative model for nonequilibrium, caused by escape of radiation, in stationary, uniform atomic nitrogen where $8000 \leq T_e \leq 15\,000$K and $10^{12} \leq N_t \leq 10^{18}$ cm^{-3}. Such conditions are close to conditions in many applications (electrical discharges, light sources, plasma processing, arcs in high-power electric thrusters, hypersonic flows, etc.) and they correspond to situations in which the plasma is *partially ionized,* i.e., when the electron density is much lower than the atomic density. At higher temperatures the plasmas become *highly ionized* and the ionic inelastic processes (not included in this work) must be considered (see Ref. 1). The model will allow for a reliable interpretation of related experiments on atomic physics and plasma diagnostics. For example, the lack of such a model has been one of the main sources of difficulties in interpretation of measurements of cross sections for electron inelastic collisions with nitrogen atoms.[2,3] In particular, the contribution of different transitions to production of radiation being measured must be known with a reasonable accuracy. This requires reliable cross sections and Einstein coefficients for the inelastic processes considered in the model. Therefore a substantial part of this work has been devoted to the determination of the best possible atomic cross sections and Einstein coefficients.

Earlier models[1,4–7] of the nonequilibrium nitrogen were linear models neglecting dielectronic recombination and the dependence of the radiation reabsorption on plasma conditions. In addition, those models were using popular, but often unrealistic, predictions for many of the atomic cross sections and Einstein coefficients. Unfortunately, the predictions are not able to provide a sufficient differentiation (reaching beyond the impact-energy dependence and the energy-threshold dependence) between (a) collisions involving metastable levels and collisions involving radiative levels, and (b) collisions with small energy thresholds and collisions with large energy thresholds. It should be emphasized that these differences are of fundamental importance in the plasmas considered here because of properties of the electronic structure of nitrogen atom. For example, the two lowest excited levels in nitrogen atom, $2s^2 2p^3\,{}^2D^\circ$ and $2s^2 2p^3\,{}^2P^\circ$, are metastable, with the radiative lifetimes equal to about 10^5 and 10^2 sec, respectively, and with low excitation energies (2.38 and 3.58 eV, respectively). The atoms excited to the metastable levels are strongly collisionally coupled with the ground state and they form a large reservoir of particles that can be ionized much more easily than the ground-state atoms. Also, the metastable atoms play a crucial role in production of the upper radiative levels. Therefore the inelastic processes involving metastable and radiative levels must be treated in a correct (i.e., different) way, as prescribed by quantum-mechanical theories of the atomic transitions.

In general, a consistent collisional-radiative model for steady-state gas should be able to determine (1) the particle energy distributions, (2) the production of plasma particles including excited species, and (3) the production and transport of radiation within the plasma. Thus the model should consist of three groups of equations coupled together: (i) a set of Boltzmann transport equations for the plasma particles, solution of which will yield the particle distribution functions; (ii) a set of rate equations for the production of electrons and the excited atoms; and (iii) the radiative-transport equation describing the transport of radiation in the plasma. Solution of these equations would yield a complete information about plasma microscopic properties (particle densities and temperatures, energy distributions, intensities of the spectral lines, etc.). Since solution of such a complex model is a very difficult task, we reduce the number of the equations by making some physically justified assumptions. In the plasmas considered here, the ionization degree is not small and Coulomb collisions play a role in redistributing the electron energy. Also, the first two excited levels of nitrogen atoms are not coupled radiatively with the ground state. Therefore deviation of the electron-energy distribution from Maxwellian, caused mainly by the electron collisions with these levels,[8,9] is rather small in the temperature range considered in this work; the energy escaping from the plasma in form of radiation (forbidden lines) produced by these levels is negligible in comparison with the energy of the electrons. Thus one can assume that the electron-energy distribution is Maxwellian. In

addition, the atom-atom and ion-atom inelastic collisions can be neglected[10,11] so that the forms of the energy distributions for ions and atoms are not important.

The rate equations for production of electrons and the excited atoms take into account the following inelastic processes: (1) electron-impact excitation, deexcitation and ionization of atoms, and three-body recombination and (2) photoexcitation, spontaneous emission, photoionization, and dielectronic and radiative recombination. We do not include atom-wall interactions because it would limit our model to a specific plasma-wall systems. In addition, atom-wall interactions are still poorly understood and their rate coefficients are often inaccurate.

The reabsorption of radiation is taken into account by using the concept of the radiation escape factors,[12] which represent the ability of the plasma to reabsorb radiation produced in the plasma. For example, the escape factor κ_{ji} for the transition from an atomic level j to a lower level i is defined by

$$N_j(r)A_{ji}\kappa_{ji}=N_j(r)A_{ji} - N_i(r)B_{ij}\left[1-\frac{N_j(r)B_{ji}}{N_i(r)B_{ij}}\right]\frac{4\pi}{c} \times\int I_{ji}(r,\nu)\phi_{ij}(\nu)d\nu\ , \tag{1}$$

where N_j is the density of the atoms excited to the jth electronic level and B_{ij} and B_{ji} are Einstein coefficients for absorption and induced emission, respectively; I_{ji} is the radiation intensity and ϕ_{ij} is the line profile. In general, the values of the escape factors are between zero (when the plasma is optically thick for the line) and 1 (when the plasma is optically thin for the line). The number of photons produced by $j\rightarrow i$ spontaneous emission, per unit volume and per unit time, is equal to $N_j A_{ji}$. $N_j A_{ji}\kappa_{ji}$ of these photons leaves the plasma while the rest of the photons $[N_j A_{ji}(1-\kappa_{ji})]$ are reabsorbed. Thus the escape factor for a line is the average probability that the photons of the line will escape from the plasma volume. In the first-order approximation the escape factors can be treated as constants, which makes the system of the rate equations linear. In the more realistic case considered in this work, the escape factors depend on plasma conditions. Then, the rate equations for the production of electrons and the excited atoms become nonlinear. Such a nonlinear system is solved here with the radiation escape factors calculated in the way discussed below.

Solution of our stationary, collisional-radiative model has established the following properties of uniform atomic nitrogen plasma in nonequilibrium: (a) the production of electrons and excited atoms as a function of plasma temperature and density, (b) the deviation of the excited atom populations from thermal equilibrium, (c) the intensities of bound-bound, dielectronic and continuum lines, (d) the contribution of photoabsorption to the production of electrons and excited atoms, and (e) the relaxation times for the atomic levels.

II. ATOMIC MODEL

Electronic energy structure assumed for atomic nitrogen is shown in Fig. 1. Each of the atomic terms (called hereafter levels) are numbered sequentially, with $i=1$ for the electronic ground state, $i=2$ for the first excited level, etc. In general, the interaction between the atomic electrons in nitrogen atom can be approximated by an LS-coupling scheme. In addition to the usual assignment of quantum numbers n, l, L, and S, all the atomic terms have also the spin (S_p) and orbital (L_p) angular momentum numbers of the corresponding atomic "cores." The ground ionic term $2s^2 2p^2\,{}^3P$ is taken as the "core" for all atoms.

The 14 atomic levels assumed in the present calculations provide a good representation of the atomic properties in the collisional-radiative model. We tested this statement by performing calculations for $n_{\max}=6$, 10, and 14 levels. A comparison of the results shows that assuming the 14 atomic levels in the model is sufficient for a reliable prediction, under the conditions considered in this work, of (a) the electron and the excited atom densities and (b) the production of the plasma radiation.

One may add that the six-level model can be used in kinetic analyses of atomic nitrogen if high accuracy is not required. For example, the differences (in the electron and excited atom densities and in the total plasma radiation) between the results of the six-level model and the 14-level model are within a half an order of magnitude.

III. COLLISIONAL-RADIATIVE MODEL

In a uniform plasma, where the atom-atom inelastic collisions are neglected, the net production of the excited atoms can be determined by balancing all inelastic processes populating and depopulating each atomic level. Similarly, the electron density can be determined by balancing all the processes leading to atomic ionization and recombination. Thus the net production rates for atoms excited to the ith level and for plasma electrons can be given, respectively, by[13]

$$\frac{\partial N_i}{\partial t}=\sum_{k\,(<i)}N_e N_k C_{ki}+\sum_{j\,(>i)}N_e N_j R_{ji}+\sum_{j\,(>i)}N_j A_{ji}\kappa_{ji} +N_e N_+(\alpha_{ci}^R\kappa_{ci}+\alpha_i^D\langle\kappa_{ai}\rangle+N_e\beta_{ci}) -N_i\left[\sum_{j\,(>i)}N_e C_{ij}+\sum_{k\,(<i)}N_e R_{ik} +\sum_{k\,(<i)}A_{ik}\kappa_{ik}+N_e S_{ic}\right] \tag{2}$$

and

$$\frac{\partial N_e}{\partial t}=\sum_i N_e N_i S_{ic}-\sum_i N_e N_e N_+\beta_{ci} -\sum_i N_e N_+(\alpha_{ci}^R\kappa_{ci}+\alpha_i^D\langle\kappa_{ai}\rangle)\ , \tag{3}$$

where N_e and N_+ are electron and ground-state ion densities, respectively. The quantities C_{ij} and R_{ji} are the rate coefficients for the electron-impact excitation and deexcitation, respectively; A_{ji} is the transition probability (Einstein coefficient) for the $j\rightarrow i$ radiative transition; S_{ic} is the electron-impact rate coefficient for ionization of the atom excited to the ith level; α_{ci}^R and β_{ci} are rate

coefficients for radiative and three-body recombination, respectively, producing an atom excited to the ith level; α_i^D is the effective dielectronic recombination rate coefficient for dielectronic transitions to the $i=1$, 2, and 3 "terminating" levels (see discussion below); κ_{ji}, κ_{ci}, and $\langle \kappa_{ai} \rangle$ are radiation escape factors, discussed below, for bound-bound, free-bound, and dielectronic radiation, respectively.

In a steady state, Eq. (2) can be rewritten as[14]

$$N_i = \frac{N_e \sum_{k(<i)} N_k C_{ki}}{\sum_{k(<i)} A_{ik}\kappa_{ik} + N_e \sum_{k(<i)} R_{ik}} + \delta_i , \tag{4}$$

where

$$\delta_i = \frac{N_e \sum_{j(>i)} (N_j R_{ji} - N_i C_{ij}) + \sum_{j(>i)} N_j A_{ji}\kappa_{ji} + N_e[N_+(\alpha_{ci}^R \kappa_{ci} + \alpha_i^D \langle \kappa_{ai} \rangle + N_e \beta_{ci}) - N_i S_{ic}]}{\sum_{k(<i)} A_{ik}\kappa_{ik} + N_e \sum_{k(<i)} R_{ik}} \tag{5}$$

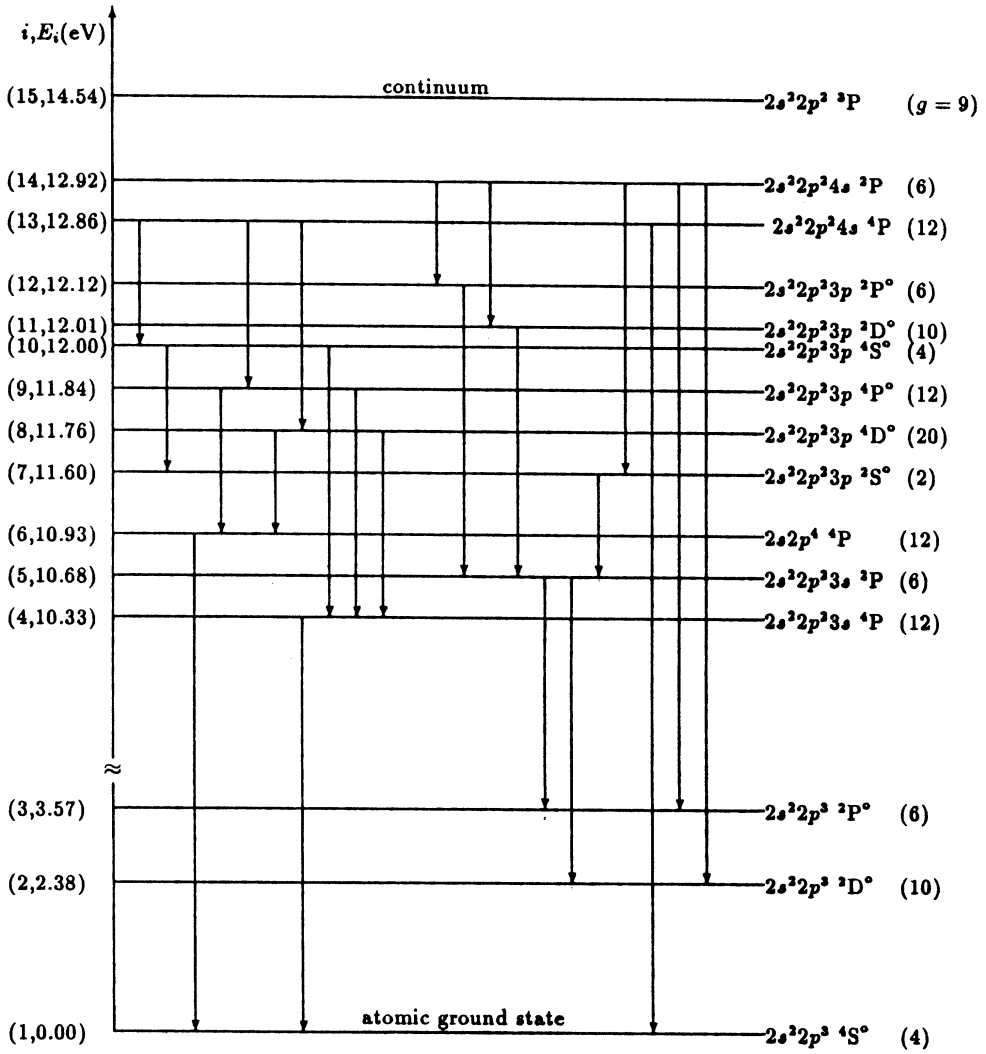

FIG. 1. Energy levels of the nitrogen atom assumed in the present work. Energies E_i of the levels (not to scale) are measured with respect to the ground state ($i=1$) and g denotes the statistical weights of the levels. The vertical arrows indicate the electric dipole-allowed transitions.

is negligible if

$$N_e \sum_{k\,(<i)} N_k C_{ki} \gg N_e \sum_{j\,(>i)} (N_j R_{ji} - N_i C_{ij}) + \sum_{j\,(>i)} N_j A_{ji} \kappa_{ji} + N_e [N_+ (\alpha_{ci}^R \kappa_{ci} + \alpha_i^D \langle \kappa_{ai} \rangle + N_e \beta_{ci}) - N_i S_{ic}] \,. \quad (6)$$

The density of atoms excited to the ith level can be obtained from Eq. (4) in a convenient Boltzmann-like form

$$\frac{N_i}{N_1} = B_i \frac{g_i}{g_1} \exp\left[-\frac{E_i - E_1}{kT_e} \right] = B_i F_i \,, \quad (7)$$

where $E_i - E_1$ is the energy gap between the ith level and the ground state, and g_i is the statistical weight of the level i. If the condition (6) is met, B_i can be given as ($B_1 = 1$)

$$B_i = \frac{\sum_{k\,(<i)} B_k \tau_{ik}}{1 + \sum_{k\,(<i)} \tau_{ik}} \quad \text{for } i > 1 \,, \quad (8)$$

with

$$\tau_{ik} = \frac{N_e R_{ik}}{\sum_{k\,(<i)} A_{ik} \kappa_{ik}} \,. \quad (9)$$

Similarly, analysis of the ionization and recombination balance in steady state [Eq. (3)] leads to the Saha-like equation[15]

$$\frac{N_+ N_e}{N_1} = H_{n_{\max}} \left[\frac{g_e g_+}{g_1} \left[\frac{2\pi m_e k T_e}{h^2} \right]^{3/2} \exp\left[-\frac{U_1}{kT_e} \right] \right] = \frac{H_{n_{\max}}}{G_1} \,, \quad (10)$$

where

$$H_{n_{\max}} = \frac{\sum_{i=1}^{n_{\max}} B_i \Upsilon_i}{1 + \sum_{i=1}^{n_{\max}} \Upsilon_i} \,, \quad (11)$$

and

$$\Upsilon_i = \frac{N_e \beta_{ci}}{\sum_{k=1}^{n_{\max}} (\alpha_k^R \kappa_{ck} + \alpha_k^D \langle \kappa_{ak} \rangle)} \,. \quad (12)$$

Here, g_+ and g_e are statistical weights of the ion and electron, respectively, U_1 is the ionization potential for the ground atomic state, $n_{\max}$ is the number of the energy levels taken into account, and the coefficients $\alpha_{k>3}^D = 0$.

Assuming charge neutrality, one can determine the atomic densities N_i from Eqs. (7) and (10). However, in some cases, the requirement (6) is violated. Therefore we obtain the solution for the steady-state population N_i from the rate equations (2) as

$$N_i = \frac{N_e \sum_{k\,(<i)} N_k C_{ki} + N_e \sum_{j\,(>i)} N_j R_{ji} + \sum_{j\,(>i)} N_j A_{ji} \kappa_{ji} + N_e N_+ (\alpha_{ci}^R \kappa_{ci} + \alpha_i^D \langle \kappa_{ai} \rangle + N_e \beta_{ci})}{N_e \left[\sum_{k\,(<i)} R_{ik} + \sum_{j\,(>i)} C_{ij} + S_{ic} \right] + \sum_{k\,(<i)} A_{ik} \kappa_{ik}} \,. \quad (13)$$

Dividing the above by N_1 and the Boltzmann factor F_i, the general expression for B_i ($B_1 = 1$) is

$$B_i = \frac{N_e \sum_{k\,(<i)} B_k F_k C_{ki} + N_e \sum_{j\,(>i)} B_j F_j R_{ji} + \sum_{j\,(>i)} B_j F_j A_{ji} \kappa_{ji} + (H_{n_{\max}} / G_1)(\alpha_{ci}^R \kappa_{ci} + \alpha_i^D \langle \kappa_{ai} \rangle + N_e \beta_{ci})}{F_i \left[N_e \left[\sum_{k\,(<i)} R_{ik} + \sum_{j\,(>i)} C_{ij} + S_{ic} \right] + \sum_{k\,(<i)} A_{ik} \kappa_{ik} \right]} \,. \quad (14)$$

The value of B_i is then iterated from Eq. (14), using B_i of Eq. (8) as an initial guess; subsequently, the value of $H_{n_{\max}}$ in Eq. (11) is corrected.

IV. EXCITATION CROSS SECTIONS AND RATE COEFFICIENTS

The main theoretical approach used here for calculation of the excitation cross sections and rate coefficients is that formulated by Vainshtein and his co-workers.[16,17] Their formalism uses the Bates-Damgaard electron radial wave functions to derive the Born cross sections σ_{ij}. The electron-atom interaction is reduced to the interaction between the incident electron and an optical electron of the target atom, the latter being in the field of the atomic core consisting of the nucleus and the other atomic electrons. Since the energy of the electronic electrostatic interactions in light atoms is much greater than the energy of the spin-orbit interactions, the LS-coupling scheme for the angular momenta is used for the description of the properties of the excited states considered in this paper.

The general form of the electron-impact cross section for a bound-bound or bound-free transition from an initial atomic term γ_i to a final term γ_j (where γ_i represents sets of quantum numbers n, l, L, S,L_p, and S_p characterizing the ith atomic term) is given in the Vainshtein approach as[16]

$$\sigma_{\gamma_i \gamma_j}^{\text{tot}}(\varepsilon) = \sum_{k_{\min}}^{k_{\max}} [Q_k' \sigma_{\gamma_i \gamma_j}'(\varepsilon, l_i, l_j) + Q_k'' \sigma_{\gamma_i \gamma_j}''(\varepsilon, l_i, l_j)] \,, \quad (15)$$

where ε is the energy of the incident electron. The single prime denotes the contribution due to direct and interference parts of the excitation and the double prime denotes the contribution due to pure exchange. $\sigma'_{\gamma_i\gamma_j}(\varepsilon,l_i,l_j)$ and $\sigma''_{\gamma_i\gamma_j}(\varepsilon,l_i,l_j)$ are cross sections for the optical electron transition $n_il_i \rightarrow n_jl_j$ (n and l being principal and orbital angular momentum quantum numbers, respectively), and Q'_k and Q''_k are angular factors that depend only on the angular momenta of the initial (γ_i) and final (γ_j) quantum states of the atom. Values of the subscript k are between $k_{\min}=|l_i-l_j|$ and $k_{\max}=|l_i+l_j|$. In the first case (single prime), k represents the multipole order for the transition, hence $\sigma'_{\gamma_i\gamma_j}$ differs from zero only for k of the same parity. In the second case (double prime), k is just the summing index of arbitrary parity.

Several transitions (called hereafter "difficult" transitions), involving excitation of two atomic electrons, cannot be treated by the Vainshtein approach (see discussion below).

The rate coefficients for electron-impact atomic excitation are defined as

$$C_{ij}(T_e)=\frac{8\pi}{m_e^2}\int_{\Delta E_{ij}}^{\infty}\varepsilon f_M(\varepsilon)\sigma_{ij}(\varepsilon)d\varepsilon\ , \tag{16}$$

where $f_M(\varepsilon)$ is the electron Maxwellian distribution

$$f_M(\varepsilon)=\left[\frac{m_e}{2\pi kT_e}\right]^{3/2}\exp\left[-\frac{\varepsilon}{kT_e}\right]\ . \tag{17}$$

Assuming the distribution (17), the principle of detailed balance is applied to obtain the deexcitation rate coefficients,

$$R_{ji}=\frac{g_i}{g_j}\exp\left[\frac{E_j-E_i}{kT_e}\right]C_{ij}\ . \tag{18}$$

A. Electron-impact excitation with $|\Delta S|=0$

1. $2\rightarrow 3$ transition

The cross section for the $2\rightarrow 3$ transition was taken from the close-coupling calculations of Henry, Burke, and Sinfailam[18] (their results seem to be more accurate than those obtained earlier by Smith *et al.*[19,20] and Seaton[21]).

2. Other transitions

All the $|\Delta S|=0$ transitions, except the $2\rightarrow 3$ transition, are calculated by using the Vainshtein approach.[16] Only the direct excitation part of the total cross section is considered for the transitions since the contribution due to exchange is negligible.

The following analytical formula, fitting the results of theoretical calculations, is used for the rate coefficients for the electron-impact atomic excitation:

$$C_{ij}(\beta)=10^{-8}\left[\frac{\mathcal{R}U_j}{\Delta E_{ij}U_i}\right]^{3/2}\frac{Q_k}{2l_i+1}\exp(-\beta)G_k(\beta)\ , \tag{19}$$

in $\mathrm{cm^3\,s^{-1}}$, where the sum in Eq. (15) has been reduced to the first term with nonzero Q_k ($k=k_{\min}$ or $k_{\min+2}$) because the higher-order cross sections are negligible. The function $G_k(\beta)$ is

$$G_k(\beta)=\frac{A\sqrt{\beta(\beta+1)}}{\beta+\chi}\ln(16+1/\beta),\quad k=1 \tag{20}$$

$$G_k(\beta)=\frac{A\sqrt{\beta(\beta+1)}}{\beta+\chi},\quad k\neq 1 \tag{21}$$

where

$$\beta=\frac{\Delta E_{ij}}{kT_e}\ , \tag{22}$$

with the parameters A and χ compiled in Table I. We assume that the interaction energy of the optical electron with electrons in the atomic core is considerably less than

TABLE I. Parameters in the rate coefficients for electron-impact excitation ($|\Delta S|=0$ transitions) of atomic nitrogen. The designation of the inner shell $1s^2$ is omitted in all electronic configuration in all tables.

$i\rightarrow j$	Transition	A	χ
1→4	$2s^22p^3\,^4S^\circ\rightarrow 2s^22p^23s\,^4P$	2.62	0.12
1→6	$2s^22p^3\,^4S^\circ\rightarrow 2s2p^4\,^4P$	6.483	0.442
1→8	$2s^22p^3\,^4S^\circ\rightarrow 2s^22p^23p\,^4D^\circ$	0.101	0.033
1→10	$2s^22p^3\,^4S^\circ\rightarrow 2s^22p^23p\,^4S^\circ$	0.231	0.081
1→13	$2s^22p^3\,^4S^\circ\rightarrow 2s^22p^24s\,^4P$	0.155	0.731
2→5	$2s^22p^3\,^2D^\circ\rightarrow 2s^22p^23s\,^2P$	0.134	0.241
2→7	$2s^22p^3\,^2D^\circ\rightarrow 2s^22p^23p\,^2S^\circ$	0.979	1.218
2→11	$2s^22p^3\,^2D^\circ\rightarrow 2s^22p^23p\,^2D^\circ$	1.784	0.793
2→12	$2s^22p^3\,^2D^\circ\rightarrow 2s^22p^23p\,^2P^\circ$	0.019	0.316
2→14	$2s^22p^3\,^2D^\circ\rightarrow 2s^22p^24s\,^2P$	0.132	0.487
3→5	$2s^22p^3\,^2P^\circ\rightarrow 2s^22p^23s\,^2P$	0.222	0.232
3→11	$2s^22p^3\,^2P^\circ\rightarrow 2s^22p^23p\,^2D^\circ$	0.167	0.373
3→12	$2s^22p^3\,^2P^\circ\rightarrow 2s^22p^23p\,^2P^\circ$	1.762	0.779
3→14	$2s^22p^3\,^2P^\circ\rightarrow 2s^22p^24s\,^2P$	0.139	0.307
4→6	$2s^22p^23s\,^4P\rightarrow 2s2p^4\,^4P$	2.424	0.977
4→8	$2s^22p^23s\,^4P\rightarrow 2s^22p^23p\,^4D^\circ$	5.467	0.659
4→9	$2s^22p^23s\,^4P\rightarrow 2s^22p^23p\,^4P^\circ$	5.528	0.622
4→10	$2s^22p^23s\,^4P\rightarrow 2s^22p^23p\,^4S^\circ$	5.563	0.549
4→13	$2s^22p^23s\,^4P\rightarrow 2s^22p^24s\,^4P$	2.679	1.149
5→7	$2s^22p^23s\,^2P\rightarrow 2s^22p^23p\,^2S^\circ$	4.409	0.829
5→11	$2s^22p^23s\,^2P\rightarrow 2s^22p^23p\,^2D^\circ$	5.373	0.611
5→12	$2s^22p^23s\,^2P\rightarrow 2s^22p^23p\,^2P^\circ$	5.413	0.550
5→14	$2s^22p^23s\,^2P\rightarrow 2s^22p^24s\,^2P$	3.126	1.121
6→8	$2s2p^4\,^4P\rightarrow 2s^22p^23p\,^4D^\circ$	4.439	0.818
6→9	$2s2p^4\,^4P\rightarrow 2s^22p^23p\,^4P^\circ$	4.776	0.773
6→10	$2s2p^4\,^4P\rightarrow 2s^22p^23p\,^4S^\circ$	5.129	0.676
7→11	$2s^22p^23p\,^2S^\circ\rightarrow 2s^22p^23p\,^2D^\circ$	1.438	1.279
7→14	$2s^22p^23p\,^2S^\circ\rightarrow 2s^22p^24s\,^2P$	0.442	0.154
8→9	$2s^22p^23p\,^4D^\circ\rightarrow 2s^22p^23p\,^4P^\circ$	0.054	0.485
8→10	$2s^22p^23p\,^4D^\circ\rightarrow 2s^22p^23p\,^4S^\circ$	0.567	0.907
8→13	$2s^22p^23p\,^4D^\circ\rightarrow 2s^22p^24s\,^4P$	0.867	0.231
9→13	$2s^22p^23p\,^4P^\circ\rightarrow 2s^22p^24s\,^4P$	0.990	0.251
10→13	$2s^22p^23p\,^4S^\circ\rightarrow 2s^22p^24s\,^4P$	1.357	0.320
11→12	$2s^22p^23p\,^2D^\circ\rightarrow 2s^22p^23p\,^2P^\circ$	0.246	0.324
11→14	$2s^22p^23p\,^2D^\circ\rightarrow 2s^22p^24s\,^2P$	1.107	0.267
12→14	$2s^22p^23p\,^2P^\circ\rightarrow 2s^22p^24s\,^2P$	1.393	0.319

the energy of the interaction among the core electrons. The energy of the atomic system is then composed of the energy of the electrons from the atomic core and the energy of the optical electron moving in the field of the core. The conservation of the core orbital ($\mathbf{L}_p$) and spin ($\mathbf{S}_p$) angular momenta implies the conservation of the total atomic orbital ($\mathbf{L}$) and spin ($\mathbf{S}$) angular momenta as well. As a result, the angular factors $Q_k(\gamma_i,\gamma_j)$ for transitions between atomic levels can be given as follows.

(i) Transitions not involving groups of equivalent electrons:

$$Q_k(\gamma_i,\gamma_j)=(2l_i+1)(2L_j+1)\begin{Bmatrix} l_i & L_i & L_p \\ L_j & l_j & k \end{Bmatrix}^2 , \quad (23)$$

where $\{\ \}$ are the $6j$ symbols for angular momentum vector addition.

(ii) Excitation from a shell of equivalent electrons:

$$Q_k(\gamma_i,\gamma_j)=m(G^{L_iS}_{L_pS_p})^2(2l_i+1)(2L_j+1) \times\begin{Bmatrix} l_i & L_i & L_p \\ L_j & l_j & k \end{Bmatrix}^2 , \quad (24)$$

where $G^{L_iS}_{L_pS_p}$ is the fractional parentage coefficient of the atomic core (parent ion) term L_pS_p.

(iii) Transitions between two different groups of equivalent electrons $l_0^N l_1^m \rightarrow l_0^{N-1} l_1^{m+1}$:

$$Q_k(\gamma_i,\gamma_j)=(4l_j+2-m)(G^{L_iS}_{L_pS_p})^2(2l_i+1)(2L_j+1) \times\begin{Bmatrix} l_i & L_j & L_p \\ L_i & l_j & k \end{Bmatrix}^2 . \quad (25)$$

(iv) Transitions between terms of the same configuration:

$$Q_k(\gamma_i,\gamma_j)=\frac{(2l_i+1)}{(2L_i+1)}|(l_i^m L_i S\|U^k\|l_i^m L_j S)|^2 , \quad (26)$$

where the matrix element for the transition is

$$(l_i^m L_i S\|U^k\|l_i^m L_j S) =m\sum_{L_pS_p}[G^{L_iS}_{L_pS_p}G^{L_jS}_{L_pS_p}(-1)^{L_p+k-l_i-L_i}] \times\sqrt{(2L_i+1)(2L_j+1)}\begin{Bmatrix} l_i & L_i & L_p \\ L_j & l_i & k \end{Bmatrix} , \quad (27)$$

and

$$(l^m L_i S\|U^k\|l^m L_j S)=-(l^{R-m}L_i S\|U^k\|l^{R-m}L_j S) , \quad (28)$$

with $R=2(2l+1)$.

The dependence of the rate coefficients for transitions between closely spaced levels (those with $\Delta E_{ij} \ll U_i, U_j, kT_e$) on ΔE_{ij} is weak. In such cases it is more convenient to express the rate coefficients by

$$C_{ij}(\beta)=10^{-8}\frac{A_1\beta_1^{1/2}}{(2l_i+1)(1+\beta_1/\chi_1)} , \quad (29)$$

in $\mathrm{cm}^3\,\mathrm{s}^{-1}$, and

$$\beta_1=\frac{\mathcal{R}}{kT_e} , \quad (30)$$

with the modified fitting parameters

$$A_1=\frac{A\mathcal{R}}{\chi\Delta E_{ij}},\quad \chi_1=\frac{\chi\mathcal{R}}{\Delta E_{ij}} . \quad (31)$$

B. Electron-impact excitation with $|\Delta S|=1$

1. $1\rightarrow 2$ and $1\rightarrow 3$ transitions

The electron-impact cross sections for the $1\rightarrow 2$ and $1\rightarrow 3$ transitions were taken from the close-coupling calculations of Henry, Burke, and Sinfailam.[18]

2. Other transitions

For the collisional model assumed, the exchange between the optical electron and the incident electron is the only possible mechanism for change in the total atomic spin. Cross sections for all the $|\Delta S|=1$ intercombination transitions, except for the two cases mentioned above, are obtained from the Vainshtein approach when only pure exchange [the second term in Eq. (15)] is considered. The rate coefficients are given in a numerically fitted form as products of angular and radial factors,

$$C''_{ij}(\beta)=10^{-8}\left[\frac{\mathcal{R}U_j}{\Delta E_{ij}U_i}\right]^{3/2}\frac{Q''}{2l_i+1}\exp(-\beta)G''(\beta) , \quad (32)$$

in $\mathrm{cm}^3\,\mathrm{s}^{-1}$, where k has disappeared because it is either single valued or is summed over all its values [Eq. (15)]; for $|\Delta S|=1$ transitions

$$k=|l_i-l_j|,|l_i-l_j|+1,\ldots,|l_i+l_j| . \quad (33)$$

The function $G''(\beta)$ is

$$G''(\beta)=\frac{A''\beta}{(\beta+\chi'')}\left[\frac{\beta}{\beta+1}\right]^{1/2} , \quad (34)$$

where the parameters A'' and χ'' are given in Table II. The angular factors Q'', summed over the multipole order k, for transitions between a lower term γ_i and an upper term γ_j, are as follows.

(i) Transitions not involving groups of equivalent electrons:

$$Q''(\gamma_i,\gamma_j)=\sum_k\frac{2S_j+1}{2(2S_p+1)}(2l_i+1)(2L_j+1) \times\begin{Bmatrix} l_i & L_i & L_p \\ L_j & l_j & k \end{Bmatrix}^2 =\frac{2S_j+1}{2(2S_p+1)} . \quad (35)$$

(ii) Transitions from shells of equivalent electrons:

$$Q''(\gamma_i,\gamma_j)=\sum_k m(G^{L_iS_i}_{L_pS_p})^2\frac{2S_j+1}{2(2S_p+1)} \times(2l_i+1)(2L_j+1)\begin{Bmatrix} l_i & L_i & L_p \\ L_j & l_j & k \end{Bmatrix}^2 =m(G^{L_iS_i}_{L_pS_p})^2\frac{2S_j+1}{2(2S_p+1)} . \quad (36)$$

The rate coefficients for the transitions between closely spaced levels are given in the following form:

TABLE II. Parameters in the rate coefficients for electron-impact excitation ($|\Delta S|=1$ transitions) of atomic nitrogen.

$i\rightarrow j$	Transition	A''	χ''
1→5	$2s^22p^3\,^4S^\circ\rightarrow 2s^22p^23s\,^2P$	3.886	0.090
1→7	$2s^22p^3\,^4S^\circ\rightarrow 2s^22p^23p\,^2S^\circ$	40.648	2.739
1→11	$2s^22p^3\,^4S^\circ\rightarrow 2s^22p^23p\,^2D^\circ$	3.649	0.219
1→12	$2s^22p^3\,^4S^\circ\rightarrow 2s^22p^23p\,^2P^\circ$	3.855	0.008
1→14	$2s^22p^3\,^4S^\circ\rightarrow 2s^22p^24s\,^2P$	3.993	0.396
2→4	$2s^22p^3\,^2D^\circ\rightarrow 2s^22p^23s\,^4P$	1.263	0.031
2→6	$2s^22p^3\,^2D^\circ\rightarrow 2s2p^4\,^4P$	20.596	1.512
2→8	$2s^22p^3\,^2D^\circ\rightarrow 2s^22p^23p\,^4D^\circ$	50.966	1.958
2→9	$2s^22p^3\,^2D^\circ\rightarrow 2s^22p^23p\,^4P^\circ$	40.559	2.547
2→10	$2s^22p^3\,^2D^\circ\rightarrow 2s^22p^23p\,^4S^\circ$	19.128	1.643
2→13	$2s^22p^3\,^2D^\circ\rightarrow 2s^22p^24s\,^4P$	4.354	0.397
3→4	$2s^22p^3\,^2P^\circ\rightarrow 2s^22p^23s\,^4P$	1.084	0.019
3→6	$2s^22p^3\,^2P^\circ\rightarrow 2s2p^4\,^4P$	22.700	1.524
3→8	$2s^22p^3\,^2P^\circ\rightarrow 2s^22p^23p\,^4D^\circ$	67.457	0.989
3→9	$2s^22p^3\,^2P^\circ\rightarrow 2s^22p^23p\,^4P^\circ$	58.186	1.473
3→10	$2s^22p^3\,^2P^\circ\rightarrow 2s^22p^23p\,^4S^\circ$	35.964	2.656
3→13	$2s^22p^3\,^2P^\circ\rightarrow 2s^22p^24s\,^4P$	4.482	0.433
4→5	$2s^22p^23s\,^4P\rightarrow 2s^22p^23s\,^2P$	1.588	0.007
4→7	$2s^22p^23s\,^4P\rightarrow 2s^22p^23p\,^2S^\circ$	18.408	1.288
4→11	$2s^22p^23s\,^4P\rightarrow 2s^22p^23p\,^2D^\circ$	15.188	1.717
4→12	$2s^22p^23s\,^4P\rightarrow 2s^22p^23p\,^2P^\circ$	13.897	1.782
4→14	$2s^22p^23s\,^4P\rightarrow 2s^22p^24s\,^2P$	0.804	0.550
5→8	$2s^22p^23s\,^2P\rightarrow 2s^22p^23p\,^4D^\circ$	16.728	1.307
5→9	$2s^22p^23s\,^2P\rightarrow 2s^22p^23p\,^4P^\circ$	16.574	1.423
5→10	$2s^22p^23s\,^2P\rightarrow 2s^22p^23p\,^4S^\circ$	15.633	1.625
5→13	$2s^22p^23s\,^2P\rightarrow 2s^22p^24s\,^4P$	3.180	1.106
7→8	$2s^22p^23p\,^2S^\circ\rightarrow 2s^22p^23p\,^4D^\circ$	0.419	0.387
7→9	$2s^22p^23p\,^2S^\circ\rightarrow 2s^22p^23p\,^4P^\circ$	7.880	0.879
7→10	$2s^22p^23p\,^2S^\circ\rightarrow 2s^22p^23p\,^4S^\circ$	15.016	1.618
7→13	$2s^22p^23p\,^2S^\circ\rightarrow 2s^22p^24s\,^4P$	1.192	0.508
8→11	$2s^22p^23p\,^4D^\circ\rightarrow 2s^22p^23p\,^2D^\circ$	7.816	0.730
8→12	$2s^22p^23p\,^4D^\circ\rightarrow 2s^22p^23p\,^2P^\circ$	7.355	1.360
8→14	$2s^22p^23p\,^4D^\circ\rightarrow 2s^22p^24s\,^2P$	0.916	0.573
9→11	$2s^22p^23p\,^4P^\circ\rightarrow 2s^22p^23p\,^2D^\circ$	3.355	0.390
9→12	$2s^22p^23p\,^4P^\circ\rightarrow 2s^22p^23p\,^2P^\circ$	12.145	0.906
9→14	$2s^22p^23p\,^4P^\circ\rightarrow 2s^22p^24s\,^2P$	1.117	0.739
10→11	$2s^22p^23p\,^4S^\circ\rightarrow 2s^22p^23p\,^2D^\circ$	18.135	0.149
10→12	$2s^22p^23p\,^4S^\circ\rightarrow 2s^22p^23p\,^2P^\circ$	1.221	0.209
10→14	$2s^22p^23p\,^4S^\circ\rightarrow 2s^22p^24s\,^2P$	1.732	1.111
11→13	$2s^22p^23p\,^2D^\circ\rightarrow 2s^23p^24s\,^4P$	2.714	1.468
12→13	$2s^22p^23p\,^2P^\circ\rightarrow 2s^22p^24s\,^4P$	3.917	1.791
13→14	$2s^22p^24s\,^4P\rightarrow 2s^22p^24s\,^2P$	0.561	0.013

$$C''_{ij}(\beta)=10^{-8}\frac{A''_1\beta_1^{3/2}}{(2l_i+1)(1+\beta_1/\chi''_1)} , \quad (37)$$

in $cm^3\,s^{-1}$, and

$$A''_1=\frac{A''}{\chi''},\quad \chi''_1=\frac{\chi''\mathcal{R}}{\Delta E_{ij}} , \quad (38)$$

where β_1 is given in Eq. (30).

C. "Difficult" transitions

As said before, the term "difficult" is used here to denote the electron-impact transitions involving excitation of two atomic electrons. The cross sections for these transitions are calculated using the quantum-classical formulation of the binary-encounter approximation.[22] In this approximation, the exchange electron-impact cross section for atomic excitation is given as (with symbols defined in Fig. 2)

$$\sigma_{\rm exc}(\varepsilon)=\frac{\pi e^4}{\varepsilon+2U_i}\left[0.924\left\{\frac{1}{\varepsilon+U_i-\Delta E_{ij+1}}-\frac{1}{\varepsilon+U_i-\Delta E_{ij}}\right\}+\frac{2U_i}{3}\left\{\frac{1}{(\varepsilon+U_i-\Delta E_{ij+1})^2}-\frac{1}{(\varepsilon+U_i-\Delta E_{ij})^2}\right\}\right] , \quad (39)$$

where ΔE_{ij+1} is to be replaced by ε when $\Delta E_{ij}\le\varepsilon<\Delta E_{ij+1}$. In the situation when there are more than one electrons in the outer shell, the cross section (39) is to be multiplied by the number of electrons in the shell.

We use Vainshtein's rate coefficient for the 4→6

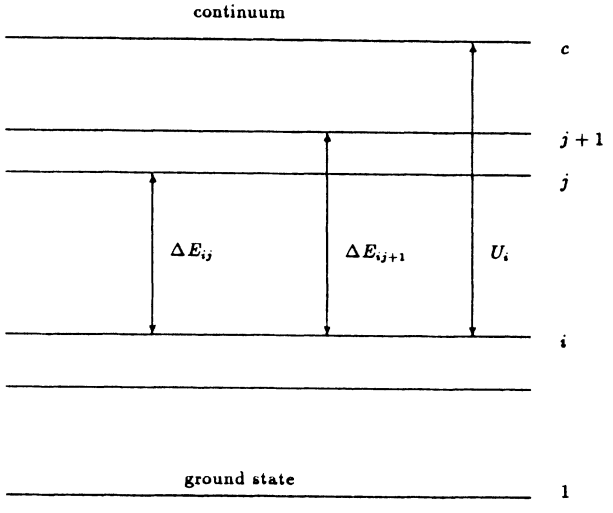

FIG. 2. Meaning of the symbols used in Eq. (39). ΔE_{ij} and ΔE_{ij+1} represent the energy gap of the $i\rightarrow j$ transition and the energy gap for excitation to the next $(j+1)$ upper level, respectively. U_i is the ionization potential for the ith level.

difficult transition. We have done so because a comparison of the binary-encounter cross section (39) for the transition with the Vainshtein cross section and with the Monte-Carlo trajectory calculations of Mansbach and Keck[23] indicated that the binary-encounter cross section is probably too high. The rate coefficients for the $6\rightarrow 8$, $6\rightarrow 9$, and $6\rightarrow 10$ transitions were also obtained from the Vainsthein approach.

V. IONIZATION CROSS SECTIONS AND RATE COEFFICIENTS

A. Experimental cross sections

The cross section used here for the electron-impact ionization from the ground state is that measured by Brook, Harrison, and Smith.[24]

B. Ionization from the two lowest excited levels

The Vainshtein approach is used to determine the rate coefficients for electron-impact ionization from the excited $2p^3$ shell (the levels $i=2$ and 3). Since these levels belong to the same shell as the atomic ground state we use the same constants A and χ for all the three levels. The constants were obtained from a numerical fitting of the ionization rate coefficient for the ground state (obtained from the cross section measured by Brook, Harrison, and Smith[24]) to the expression

$$S_{ic}(\beta)=10^{-8}\left[\frac{\mathcal{R}}{U_i}\right]^{3/2}\frac{Q_i}{2l_i+1}\exp(-\beta)G_i(\beta)\ , \tag{40}$$

in $\mathrm{cm}^3\,\mathrm{s}^{-1}$, where

$$G_i(\beta)=\left[\frac{\beta}{\beta+1}\right]^{1/2}\frac{A}{\beta+\chi}\ , \tag{41}$$

and

$$\beta=\frac{U_i}{kT_e}\ . \tag{42}$$

The parameters A and χ for the levels $i=1$, 2, and 3 are 27.71 and 5.58, respectively.

The angular factors Q_i for ionization from the outer shell l_i^3 with m electrons are

$$Q_i(l_i^m L_i S_i, l_i^{m-1} L_p S_p)=m(G_{L_p S_p}^{L_i S_i})^2\ . \tag{43}$$

The angular factor for the $i=1$ level is equal to 3 and it is equal to $\frac{3}{2}$ for the levels $i=2$ and 3.

C. Ionization from excited levels with $i>3$

The cross sections of Gryzinski and Kunc[25] are used for the electron-impact ionization of excited nitrogen atoms with $i>3$. These cross sections are in good agreement with experimental values for ionization from the ground states of various atoms and they should be an acceptable approximation for ionization from the intermediate levels considered in this work. (A more accurate version of the cross sections can be obtained by using the approach of Gryzinski and Kunc with the atomic electron distributions formulated recently by Kunc.[26]) The cross sections have the analytical form

$$\sigma_{ic}(\varepsilon)=\frac{\pi e^4}{U_i^2}\frac{m}{[(\lambda^2+k_g)^{1/2}+1]^2}\times\left[1+\frac{2}{(\lambda^2+k_g)^{1/2}}+\frac{2}{3}\left[1+\frac{1}{\lambda^2}\right]\right]\times\left[1-\frac{1}{\lambda^2}\right]\ , \tag{44}$$

where m is the number of electrons in the outer shell, U_i is the ionization potential for the level i, $\lambda^2=\varepsilon/U_i$, and $k_g=W/U_1^s$; U_1^s is the first ionization potential of the outer shell and W is the average binding energy of the electrons in the shell

$$W=\frac{1}{m}\sum_{j=1}^{m}(U_i^s)_j\ . \tag{45}$$

The three-body recombination rate coefficients are obtained from the principle of detail balance

$$\beta_{ci}=\frac{g_i}{g_e g_+}\left[\frac{h^2}{2\pi m_e kT_e}\right]^{3/2}\exp\left[\frac{U_i}{kT_e}\right]S_{ic}\ . \tag{46}$$

VI. SPONTANEOUS EMISSION

Considering the important role of radiation in the nonequilibrium plasmas, it is important to use reliable values of the Einstein coefficients A_{ji}. To calculate many of the coefficients (especially those for the intercombination transitions) one must include the possibility of strong spin-orbit magnetic interaction. A summary of the selection rules used in this work for electric dipole ($E1$), magnetic dipole ($M1$), and electric quadrupole ($E2$) transitions is given, with decreasing order of restriction, in Table III.

The probabilities for $j\rightarrow i$ transitions involving terms with fine structure are obtained as multiplet averages

$$A_{ji}=\frac{1}{\sum_{J_j}(2J_j+1)}\sum_{J_i,J_j}(2J_j+1)A_{ji}(J_j,J_i)\ . \tag{47}$$

A. Transitions with $|\Delta S|=0$

The magnetic interaction makes a negligible contribution to the oscillator strengths for the $|\Delta S|=0$ transitions[27,28] and the assumption of LS-coupling scheme is valid.

(i) Electric dipole ($E1$) lines. The Einstein coefficients for the electric dipole lines were obtained from work of various authors.[29–37] Due to the large volume of experimental and theoretical results available for the lines, only the most recent and commonly accepted Einstein coefficients are used. These coefficients are averaged and the averaged values are used in this work (Table IV).

(ii) Electric quadrupole ($E2$) lines. The oscillator

TABLE III. Selection rules used in the present work for $E1$, $M1$, and $E2$ radiation. S and L are atomic spin and orbital angular momentum quantum numbers; J and M are atomic total angular momentum and magnetic orbital momentum quantum numbers, respectively; n and l are the principal and orbital angular momentum quantum numbers for the optical electron.

	Electric dipole ($E1$)	Magnetic dipole ($M1$)	Electric quadrupole ($E2$)
(1)	$\Delta J=0,\pm1$ (except $0\not\to0$)	$\Delta J=0,\pm1$ (except $0\not\to0$)	$\Delta J=0,\pm1,\pm2$ (except $0\not\to0,\frac{1}{2}\not\to\frac{1}{2},0\not\to1$)
(2)	$\Delta M=0,\pm1$ (except $0\not\to0$ when $\Delta J=0$)	$\Delta M=0,\pm1$ (except $0\not\to0$ when $\Delta J=0$)	$\Delta J=0,\pm1,\pm2$
(3)	parity change	no parity change	no parity change
(4)	one electron jump $\Delta l=\pm1$ Δn arbitrary	no electron jump $\Delta l=0$ $\Delta n=0$	one or no electron jump $\Delta l=0,\pm2$ Δn arbitrary
		For LS coupling only	
(5)	$\Delta S=0$	$\Delta S=0$	$\Delta S=0$
(6)	$\Delta L=0,\pm1$ (except $0\not\to0$)	$\Delta L=0$	$\Delta L=0,\pm1,\pm2$ (except $0\not\to0,0\not\to1$)

strength for the $3\to2$ transition has been calculated by Butler and Zeippen[38] and this result is used here. The Einstein coefficients for electric quadrupole lines, except the difficult transitions, are calculated from Eq. (48) assuming the oscillator strength $f_{ij}=6.8\times10^{-10}$.

B. Transitions with $|\Delta S|=1$

In this case, both magnetic dipole ($M1$) and electric quadrupole ($E2$) interactions are considered. The coefficients A_{ji} (for magnetic dipole $M1$ plus electric quadrupole $E2$) averaged over the multiplet for the $2\to1$ and $3\to1$ transitions are available in literature[28,37–39] (we use in this paper the recent calculations of Butler and Zeippen[38]). The oscillator strength for the $5\to1$ and $14\to1$ transitions are taken from Ref. 30.

A simple approach, based on the results discussed above and on a survey of oscillator strengths for other intercombination lines, is used here to estimate the Einstein coefficients for the rest of the $|\Delta S|=1$ transitions. We assume values of $f_{ij}=1.1\times10^{-5}$ for lines with wavelength $\lambda_{ji}\lesssim2500$ Å and $f_{ij}=7.25\times10^{-12}$ for all lines with $\lambda_{ji}>2500$ Å. Using these values, the transition probabilities are obtained from

TABLE IV. Electric dipole ($E1$) lines in the nitrogen atom. λ_{ji}, f_{ij}, and A_{ji} are the line wavelength, absorption oscillator strength, and Einstein's coefficient, respectively.

$j\to i$	Transition	λ_{ji} (Å)	f_{ij}	A_{ji} (s^{-1})
$4\to1$	$2s^22p^23s\,^4P\to2s^22p^3\,^4S^\circ$	1199.9	2.7×10^{-1}	4.16×10^{8}
$6\to1$	$2s2p^4\,^4P\to2s^22p^3\,^4S^\circ$	1134.6	7.2×10^{-2}	1.24×10^{8}
$13\to1$	$2s^22p^24s\,^4P\to2s^22p^3\,^4S^\circ$	965.1	3.6×10^{-2}	8.7×10^{7}
$5\to2$	$2s^22p^23s\,^2P\to2s^22p^3\,^2D^\circ$	1493.3	7.0×10^{-1}	3.5×10^{8}
$14\to2$	$2s^22p^24s\,^2P\to2s^22p^3\,^2D^\circ$	1177.8	3.0×10^{-3}	2.39×10^{7}
$5\to3$	$2s^22p^23s\,^2P\to2s^22p^3\,^2P^\circ$	1743.6	6.1×10^{-2}	1.3×10^{8}
$14\to3$	$2s^22p^24s\,^2P\to2s^22p^3\,^2P^\circ$	1328.1	6.0×10^{-2}	2.27×10^{8}
$8\to4$	$2s^22p^23p\,^4D^\circ\to2s^22p^23s\,^4P$	8700.6	5.9×10^{-1}	3.1×10^{7}
$9\to4$	$2s^22p^23p\,^4P^\circ\to2s^22p^23s\,^4P$	8216.6	3.6×10^{-1}	3.57×10^{7}
$10\to4$	$2s^22p^23p\,^4S^\circ\to2s^22p^23s\,^4P$	7456.2	1.3×10^{-1}	4.56×10^{7}
$7\to5$	$2s^22p^23p\,^2S^\circ\to2s^22p^23s\,^2P$	13 544.8	9.6×10^{-2}	1.05×10^{7}
$11\to5$	$2s^22p^23p\,^2D^\circ\to2s^22p^23s\,^2P$	9406.4	5.8×10^{-1}	2.64×10^{7}
$12\to5$	$2s^22p^23p\,^2P^\circ\to2s^22p^23s\,^2P$	8628.0	3.4×10^{-1}	3.04×10^{7}
$8\to6$	$2s^22p^23p\,^4D^\circ\to2s2p^4\,^4P$	14 930.3	7.6×10^{-2}	1.37×10^{6}
$9\to6$	$2s^22p^23p\,^4P^\circ\to2s2p^4\,^4P$	13 559.6	3.1×10^{-1}	1.13×10^{7}
$10\to6$	$2s^22p^23p\,^4S^\circ\to2s2p^4\,^4P$	11 606.2	1.2×10^{-2}	1.71×10^{6}
$14\to7$	$2s^22p^24s\,^2P\to2s^22p^23p\,^2S^\circ$	9435.0	1.0	2.55×10^{7}
$13\to8$	$2s^22p^24s\,^4P\to2s^22p^23p\,^4D^\circ$	11 299.7	1.1×10^{-2}	9.59×10^{5}
$13\to9$	$2s^22p^24s\,^4P\to2s^22p^23p\,^4P^\circ$	12 235.8	4.3×10^{-2}	1.9×10^{6}
$13\to10$	$2s^22p^24s\,^4P\to2s^22p^23p\,^4S^\circ$	14 426.8	4.3×10^{-1}	4.56×10^{6}
$14\to11$	$2s^22p^24s\,^2P\to2s^22p^23p\,^2D^\circ$	13 604.2	9.2×10^{-2}	5.55×10^{6}
$14\to12$	$2s^22p^24s\,^2P\to2s^22p^23p\,^2P^\circ$	15 645.7	4.9×10^{-2}	1.32×10^{6}

$$A_{ji}=\frac{6.67\times10^{15}}{\lambda_{ji}^2}\frac{g_i}{g_j}f_{ij}\ , \tag{48}$$

with the wavelength λ_{ji} in angstroms and the Einstein coefficient in s^{-1}.

C. Difficult transitions

The value of the oscillator strength $f_{ij}=10^{-9}$ was assumed[27] for these transitions. Consequently, Eq. (48) is used to estimate the corresponding transition probabilities. This simple approach seems to give reasonable estimates of the Einstein coefficients for the $E2$ and $M1$ transitions [in any case, the possible error resulting from this approach cannot introduce any significant inaccuracy to the collisional-radiative model because the collisional deexcitation ($N_jN_eR_{ji}$) always dominates the radiative deexcitation ($N_jA_{ji}\kappa_{ji}$) in the $j\rightarrow i$ difficult transitions].

VII. DIELECTRONIC RECOMBINATION

Dielectronic recombination is a result of two-stage process: dielectronic capture (with the reverse process—autoionization) followed by radiative stabilizing transition,

$$e+X_p^+\rightarrow X_a\rightarrow X_i+h\nu\ , \tag{49}$$

where p denotes an initial state of the atomic ion X^+, a and i represent an autoionizing (doubly excited) and a "true" bound (singly excited) state of the atom X.

Nussbaumer and Storey[31,40] showed recently, including the contributions due to the outer electron, that the dielectronic recombination can be more important than the radiative recombination at temperatures below 20 000 K and that the efficiency of the process is much higher than that obtained from the Burgess formula[41,42] (see Fig. 3).

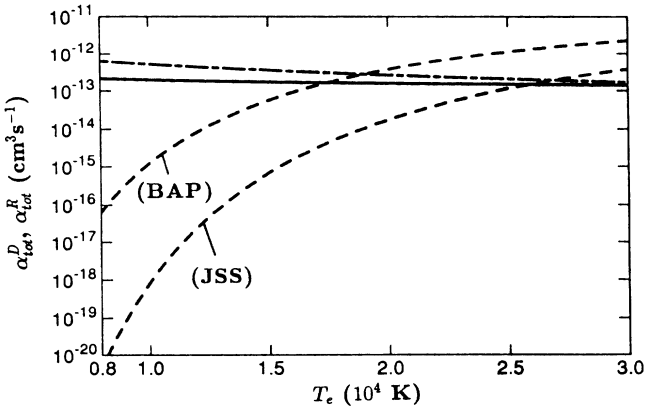

FIG. 3. Comparison of the total dielectronic recombination rate $\alpha_{\rm tot}^D=\sum_{i=1}^3\alpha_i^D$ (dot-dashed lines) and the total radiative recombination rate $\alpha_{\rm tot}^R=\sum_{i=1}^{14}\alpha_{ci}^R$ (solid line) of the present work. (BAP) represents the total dielectronic recombination rate of Aldrovandi and Pequignot (Ref. 83) based on the Burgess model neglecting stablizing transitions of the captured electron. (JSS) represents the total dielectronic recombination rate of Shull and van Steenberg (Ref. 84) based on the Jacobs model also neglecting stabilizing transitions of the captured electron.

We use here the approach of Nussbaumer and Storey (NS) assuming that the population of the excited ionic levels is much lower than the population of the ground state of the recombining ion [$p=1$ in Eq. (49)]. Since the first excited level ($2p^2\,{}^1D$) of N^+ ion is metastable and has the excitation energy about 2 eV, the assumption requires the ratio N_e/N_a to be much less than one in the plasmas discussed here. Another important assumption of the NS model is that only radiative transitions satisfying LS-coupling electric dipole selection rules are included.

It has been shown by a number of authors[43–47] that various collisional effects (collisional stablization by electrons and atoms and collisional transitions between close-lying autoionizing levels) can influence dielectronic recombination at moderate and high plasma densities. As electron density increases (from lower values) the contribution of the angular-momentum-changing electron collisions between the autoionizing levels increases most rapidly.[46,47] A crude estimate of this contribution (detailed calculations for the N^+ ion are not available in literature) can be made by comparing the rates for the angular-momentum-changing collisions with the rates for stablizing radiative transitions in the way discussed for highly charged ions by Jacobs and Blaha.[47] The comparison indicates that the angular-momentum-changing collisions become important in atomic nitrogen when $N_e\gtrsim10^{14}-10^{15}$ cm^{-3}. (Jacobs and Blaha also discussed the validity of LS-coupling approximation when these collisional processes are included.) One should add that at higher electron density ($N_e\gtrsim10^{14}$ cm^{-3}) the effect of screening the Coulomb potential of the ion by surrounding electrons and ions must be included.[44,48] The screening reduces the number of bound states, causing a decrease in the recombination coefficient. Also, at very high atomic densities the atom-stabilized transitions,[49] $e+X^++X\rightleftarrows X_i+X$, should be included. Taking the above into account, one can say that the collisional effects discussed above can be important for the dielectronic recombination in the plasmas considered here if $N_e>10^{14}-10^{15}$ cm^{-3}.

The NS approach allows one to calculate (neglecting the collisional effects discussed above) the dielectronic recombination coefficients for the effective (direct plus cascade) transitions to the "terminating" levels i (the coefficients α_i^D). The terminating levels are the metastable levels at which the cascades terminate, that is, the probability of further downward radiative transitions is very small. The effective dielectronic recombination coefficient α_i^D is defined in such a way that the rate of population (resulting from dielectronic recombination only), per unit volume and unit time, of the ith terminating level is given by

$$\frac{dN_i^D}{dt}=N_eN_+\alpha_i^D\langle\kappa_{ai}\rangle\ , \tag{50}$$

and similarly,

$$\frac{dN_e^D}{dt}=-\sum_{i=1}^{3}N_eN_+\alpha_i^D\langle\kappa_{ai}\rangle\ , \tag{51}$$

and these terms are included in the rate equations (2) and (3) when $i=1$, 2, and 3. The effective dielectronic recombination rate coefficient α_i^D can be fitted to the following expression:[31]

$$\alpha_i^D = 10^{-12}(a/t + b + ct + dt^2)t^{-3/2}\exp(-f/t) \quad (52)$$

in $cm^3 s^{-1}$, where $t = T_e(K)/10\,000$ K and the constants for the $i=1$, 2, and 3 levels are listed in Table V. The dielectronic rates α_1^D, α_2^D, and α_3^D are compared with the radiative recombination rates α_{c1}^R, α_{c2}^R, and α_{c3}^R in Fig. 4. One should add that the plasma total dielectronic recombination coefficient α_{tot}^D of the present work is very close to the sum of the coefficients α_i^D taken over the $i=1$, 2, and 3 levels. Examples of autoionizing states a and $a \rightarrow i$ direct transitions populating the $i=1$, 2, and 3 atomic levels are shown in Fig. 5.

VIII. RADIATIVE RECOMBINATION

The cross section for radiative recombination to the ith atomic level can be obtained from Milne's relation[50]

$$\sigma_{ci}(\varepsilon) = \frac{g_i}{g_e g_+}\frac{(h\nu)^2}{\varepsilon m_e c^2}\sigma_{ic}(\nu) , \quad (53)$$

where $\sigma_{ic}(\nu)$ is the photoionization cross section, ν is the continuum line frequency, and ε is the kinetic energy of the incident electron. It was established by Bates and Dalgarno[51] that direct application of the photoionization cross sections for hydrogenlike species to the low-lying states of multielectron atoms is inappropriate. The photoionization cross sections for multielectron atoms can be obtained from the formalism of Burgess and Seaton[52] and of Peach;[53-55] for a $L_p S_p nl\ LS \rightarrow L_p S_p \varepsilon' l' L' S$ transition the cross section is

$$\sigma_{ic}(\nu) = \frac{5.45\times 10^{-19} n_{\rm eff}^3}{(1+\varepsilon' n_{\rm eff}^2)^3} \times \sum_{l'=l\pm 1} C_{l'} \| G(n_{\rm eff} l; \varepsilon' l') \cos\Phi \|^2 , \quad (54)$$

in cm^2, with

$$\Phi = \pi[n_{\rm eff} + \mu_{l'}(\varepsilon') + \chi(n_{\rm eff} l; \varepsilon' l')] , \quad (55)$$

where $n_{\rm eff} = (\mathcal{R}/U_i)^{1/2}$ is the effective principle quantum number for the ith level and the ejected electron energy $\varepsilon' = h\nu - U_i$ is given in rydbergs. $\mu_{l'}(\varepsilon')$ is the quantum defect of the $l'L'$ series and it may be extrapolated to positive energy in the continuum spectrum as $\mu_{l'}(0) + b\varepsilon'$.[53,56] The functions $G(n_{\rm eff} l; \varepsilon' l')$ and $\chi(n_{\rm eff} l; \varepsilon' l')$ were calculated by Peach.[54] The values of $\mu_{l'}(0)$ and the slope b of the $l'L'$ series, obtained from calculations of Peach,[53] are summarized in Table VI. The coefficient $C_{l'}$ in Eq. (54) is

$$C_{l'} = \sum_{L'=L\pm 1} (2L'+1) \begin{Bmatrix} l & L & L_p \\ L' & l' & 1 \end{Bmatrix}^2 l_{\rm max} , \quad (56)$$

where $l_{\rm max}$ is the larger of the two numbers l and l'.

The formula (54) is also applicable to photoionization

TABLE V. Constants in the effective dielectronic recombination rate coefficients α_i^D.

i	a	b	c	d	f
1	0.0102	−0.0032	0.0754	−0.0068	3.1555
2	0.0017	0.5661	0.1008	−0.0121	0.4443
3	0.0000	0.1264	0.0273	−0.0031	0.4570

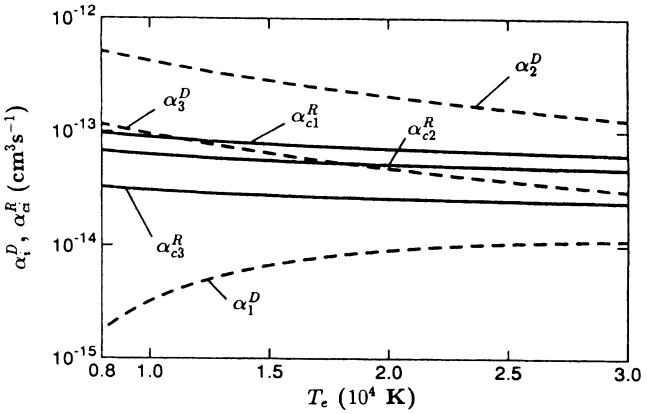

FIG. 4. T_e dependence of the effective dielectronic recombination rates α_i^D (dashed lines) and radiative recombination rates α_{ci}^R (solid lines) obtained in the present work.

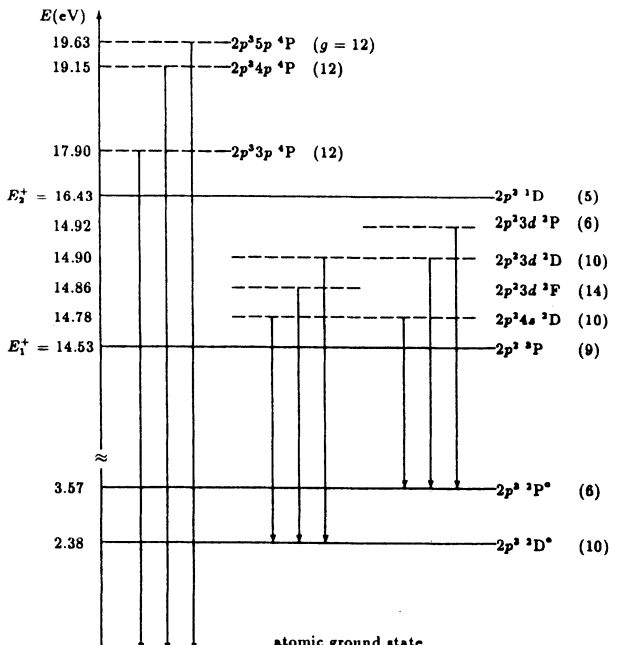

FIG. 5. Some of the $a \rightarrow i$ direct transitions, indicated by the vertical arrows, populating the "terminating" levels $i=1$, 2, and 3 in atomic nitrogen. The doubly excited autoionizing levels are represented by the dashed lines, whereas the singly excited atomic and ionic levels are represented by the solid lines. E and g are energies (not to scale) and statistical weights of the levels, respectively, and E_1^+ and E_2^+ are energies of the ground and the first excited ionic levels, respectively.

TABLE VI. Quantum-defect parameters $\mu_{l'}(\varepsilon')$ for the $l'SL'$ series.

l'	$2S+1$	L'	$\mu_{l'}(0)$	b
0	2	1	1.100	−0.080
0	4	1	1.165	0.000
1	2	0	0.798	−0.246
1	2	2	0.619	−0.361
1	4	0	0.651	−0.214
1	4	2	0.751	−0.198
2	2	1	0.067	0.000
2	2	2	0.009	0.000
2	4	1	0.030	0.000
2	4	2	0.058	0.000

from the $2p^3$ shell of the nitrogen atom ($i=1$, 2, and 3). However, we use here a simpler (but accurate) formula of Henry.[57] His photoionization cross section, based on work of Seaton[58] and Dalgarno and Parkinson,[59,60] is

$$\sigma_{ic}(\nu)=10^{-18}\sigma_{\rm th}\left[\alpha\left[\frac{\nu}{\nu_{\rm th}}\right]^{-s}+(1-\alpha)\left[\frac{\nu}{\nu_{\rm th}}\right]^{-(s+1)}\right], \tag{57}$$

in cm^2, where the photon frequency ν and the threshold frequency $\nu_{\rm th}$ are

$$\nu=\frac{U_i+\varepsilon'}{h},\quad \nu_{\rm th}=\frac{U_i}{h}. \tag{58}$$

The parameters $(\sigma_{\rm th},\alpha,s)$ for photoionization from levels $i=1$, 2, and 3 to the ground ionic state are (11.42,4.287,2.0), (4.41,3.847,1.5), and (4.20,4.337,1.5), respectively.

The radiative recombination cross sections (53) are used with the Maxwellian electron distribution to obtain the rate coefficients α_{ci}^R for radiative recombination to each atomic level i; the major contribution to the total rate comes from the recombination to the lowest levels (with $i\le 3$) since $\alpha_{ci}^R\propto\nu^2 n_{\rm eff}^{-3}$.

IX. RADIATION ESCAPE FACTORS

The line profiles $\phi_{ij}(\nu)$ assumed in the present calculations are those resulting from superposition of the Doppler and Lorentz lines (the Voigt profile). The frequency-dependent photoabsorption cross section for the $i\rightarrow j$ transition can then be given by

$$\sigma_{ij}(\nu)=\frac{\pi e^2}{m_e c}f_{ij}\phi_{ij}(\nu), \tag{59}$$

where

$$\phi_{ij}(\nu)=\frac{1}{\Delta\nu_D}\left[\frac{\ln 2}{\pi}\right]^{1/2}H(a,b), \tag{60}$$

with

$$a=\frac{\Delta\nu_L}{\Delta\nu_D}(\ln 2)^{1/2}, \tag{61}$$

$$b=\frac{(\nu-\nu_{ji})}{\Delta\nu_D}(\ln 2)^{1/2}, \tag{62}$$

and where the Voigt function $H(a,b)$ is

$$H(a,b)=\frac{a}{\pi}\int_{-\infty}^{+\infty}\frac{\exp(-y^2)dy}{a^2+(b-y)^2}, \tag{63}$$

with normalization condition

$$\int_{-\infty}^{+\infty}\phi_{ij}(\nu)d(\nu-\nu_{ji})=\frac{1}{\sqrt{\pi}}\int_{-\infty}^{+\infty}H(a,b)db=1. \tag{64}$$

The half-widths of the Lorentz and Doppler profiles are

$$\Delta\nu_L=\frac{A_{ji}}{4\pi}, \tag{65}$$

and

$$\Delta\nu_D=\frac{\nu_{ji}}{c}\left[\ln 2\left[\frac{2kT_a}{m_a}+V^2\right]\right]^{1/2}=\frac{\nu_{ji}}{c}\left[\ln 2\left[\frac{2kT_a}{m_a}\right](1+\rho^2)\right]^{1/2}, \tag{66}$$

where m_a and T_a are atomic mass and temperature, respectively, V is the most probable microturbulent flow speed of the atoms, and ρ is the ratio (neglected in the present calculations) of the microturbulent flow speed to the average thermal speed of the atoms. A_{ji}, ν_{ji}, and the atomic constants c,e,h,k,m_e have their usual meanings.

Values of the Voigt function are calculated using the numerical approach of Armstrong,[61] which leads to results in very good agreement with results of other calculations[62–64] in a wide range of the parameters a and b. One may add that numerical calculations show that under most of plasma conditions considered in this work, the Doppler profile dominates the broadening of spectral lines.

The $j\rightarrow i$ escape factor for a plane-parallel geometry of width L with a Doppler absorption profile can be given as[65,66]

$$\kappa_{ji}(\tau,\Omega)=\frac{\Omega}{1-\Omega}\left[\frac{B}{S(\tau)}-1\right], \tag{67}$$

where B is the Planck function,

$$\Omega=\frac{\eta}{1+\eta}, \tag{68}$$

$$\eta=\frac{N_e R_{ji}}{A_{ji}}\left[1-\exp\left[-\frac{h\nu_{ji}}{kT_e}\right]\right], \tag{69}$$

and the source function is related to the optical depth τ by

$$S(\tau)=(1-\Omega)\int_0^{\langle\tau\rangle}K_1(|t-\tau|)S(t)dt+\Omega B, \tag{70}$$

with

$$K_1(\tau)=\tfrac{1}{2}\int_{-\infty}^{+\infty}\phi_{ij}^2(u)\,\mathrm{Ei}_1(\tau\phi_{ij}(u))du. \tag{71}$$

The mean optical depth $\langle\tau\rangle$, defined in terms of the average absorption coefficient $\langle k(\nu)\rangle$, is

$$\langle \tau \rangle = \int_0^L \langle k(\nu) \rangle dx \ . \tag{72}$$

Otsuka, Ikee, and Ishii[65,66] derived the upper and lower limits for the escape factors from studies of the upper and lower bounds of the source function.[67] Numerical calculations of the factors $\kappa_{ji}(\langle \tau_0 \rangle = \langle \tau \rangle /2)$ at the symmetry plane of the slab ($x = L/2$) [Eq. (67)] over the range $10^{-8} \leq \Omega \leq 1$ and $10^{-3} \leq \langle \tau \rangle \leq 10^5$, consistently satisfy the two limits. In addition, at large optical depth $\langle \tau \rangle$, the functional dependence of the escape factors

$$\kappa_{ji}(\langle \tau_0 \rangle = \langle \tau \rangle /2) = \frac{1.8}{\langle \tau_0 \rangle (\pi \ln \langle \tau_0 \rangle)^{1/2}} \quad \text{for } \langle \tau \rangle > 10^5 \tag{73}$$

agrees with the asymptotic result of Holstein[12] within 10% over the $10^2 \leq \langle \tau \rangle \leq 10^5$ range. (It should be added that in our approach the $j \rightarrow i$ escape factor evaluated at the center of the uniform slab is equal to the average probability that the photons produced in the $j \rightarrow i$ transitions, in a column across the plasma slab, will reach the edge of the slab.) The escape factors are poorly sensitive to the variation of Ω. It is noteworthy that the earlier escape factors of Drawin[68] [$\kappa_{ji} \propto \exp(-\Omega \langle \tau \rangle)$] show strong dependence on Ω, violating the upper and lower limits of the escape factors used in this work.

The average absorption coefficient in uniform plasma is

$$\langle k(\nu) \rangle = N_i \langle \sigma_{ij}(\nu) \rangle \left[1 - \frac{g_i N_j}{g_j N_i} \right] , \tag{74}$$

and the mean optical depth is

$$\langle \tau \rangle = N_i \frac{\sigma_{ij}(\nu_{ji})}{2} \left[1 - \frac{g_i N_j}{g_j N_i} \right] L , \tag{75}$$

if one replaces the average absorption cross section $\langle \sigma_{ij}(\nu) \rangle$ by half of the maximum absorption cross section evaluated at the line center frequency ν_{ji}.

The radiation escape factors κ_{ai} for the dielectronic recombination lines are calculated in the way similar to that used above for the transitions between singly excited atomic levels. The effective radiation escape factors $\langle \kappa_{ai} \rangle$, used below in the calculations of the intensity of radiation produced in the dielectronic recombination to the terminating levels, were estimated from the properties of the direct, dipole-allowed dielectronic transitions ending on the ith terminating level. This is a good assumption at lower densities when the reabsorption of the dipole-allowed lines is weak and the contribution of the dielectronic radiation associated with cascades is small. At higher plasma densities the direct, dipole-allowed dielectronic lines are well reabsorbed and the contribution of the dielectronic radiation resulting from the cascades may become large enough to question the assumption. However, this contribution would not change the overall picture of plasma radiation, because at higher densities the part of the radiation produced in the $j \rightarrow i$ transitions forming the cascades that originate on the autoionizing levels is smaller than the part of the radiation produced in these transitions as the result of atomic processes other than dielectronic recombination.

The escape factors for the $c \rightarrow i$ continuum lines are calculated by assuming the exponential dependence

$$\kappa_{ci} \simeq \exp(-\langle \tau_{ci} \rangle), \quad \langle \tau_{ci} \rangle \lesssim 1 \tag{76}$$

with the average optical depth given by

$$\langle \tau_{ci} \rangle = \left[\sum_{j\ (\geq i)} N_j \sigma_{jc}(\langle \nu_i \rangle) + \sum_{k=k'}^{i-1} N_k \sigma_{kc}(\langle \nu_i \rangle) \right] L , \tag{77}$$

where the levels k ($k' \leq k \leq i-1$) are all the atomic levels lying within the energy gap $3kT_e/2$ below the ith level (see Fig. 6). The relationship (77) was obtained by assuming that most of the recombining free electrons have initial energy equal to $3kT_e/2$. Then, most of the continuum photons produced in the $c \rightarrow i$ recombination have average frequency

$$\langle \nu_i \rangle = \frac{U_i + \frac{3}{2} kT_e}{h} \ . \tag{78}$$

These continuum photons can be reabsorbed by the atoms excited to the level i and levels $j > i$ and by the atoms excited to the energy levels within the energy gap $E_i - E_k \leq 3kT_e/2$.

As the optical depth increases ($\langle \tau_{ci} \rangle > 1$), the rapid exponential decay of the κ_{ci} does not describe the free-bound continuum radiation correctly. Emission and absorption of radiation (both spectral and continuum) should be closer to balancing each other with the increase of the optical depth. At higher density, the free-bound emission in plasma slab of width L is proportional to $N_e N_+ \sigma_{ic}(\nu) L$. Therefore, for the absorption to balance the emission, the escape factors κ_{ci} should rather be

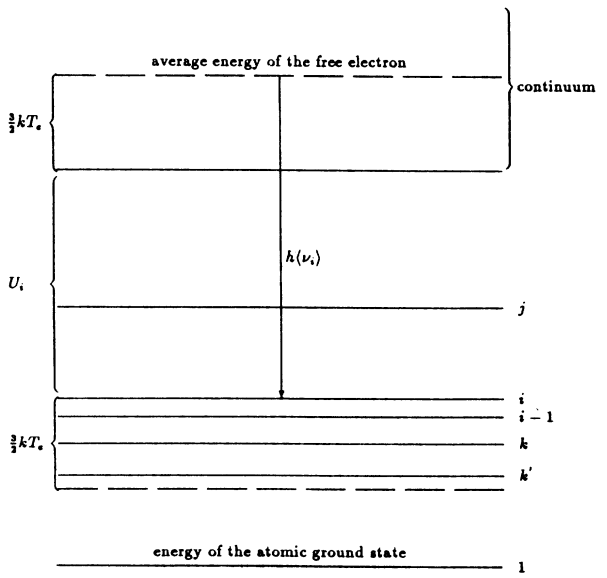

FIG. 6. Atomic levels able to reabsorb the average-energy photon $h\langle \nu_i \rangle$ produced in the $c \rightarrow i$ transitions: (a) all the levels with $j > i$, (b) the level i, and (c) all the levels k with $E_i - E_k \leq 3kT_e/2$.

$$\kappa_{ci} \propto \frac{1}{N_i \sigma_{ic}(\nu) L} \simeq \frac{1}{\langle \tau_{ci} \rangle}, \quad \langle \tau_{ci} \rangle \gg 1 \ . \tag{79}$$

X. LINE INTENSITIES

The intensity (defined as the net power radiated in all directions from a unit volume of uniform plasma slab) of the $j \rightarrow i$ spectral line in a homogeneous plasma is

$$I_{ji} = N_j A_{ji} \kappa_{ji} h \nu_{ji} \ . \tag{80}$$

It is of a spectroscopic interest to estimate the intensity of radiation, produced in a 1 cm$\times$1 cm$\times L$ column across the plasma slab, reaching the edge of the slab. This intensity, per unit solid angle, is

$$I_{ji}^{L} = \frac{I_{ji} L}{4\pi} \ , \tag{81}$$

and similarly for continuum radiation.

The total net intensity of the bound-bound atomic emission is taken as a sum over all the $j \rightarrow i$ atomic transitions,

$$I_{\rm bb} = \sum_{j} \sum_{i\,(<j)} I_{ji} \ . \tag{82}$$

The line intensity ratio of two radiative transitions $j \rightarrow i$ (with frequency ν_{ji}) and $m \rightarrow l$ (with frequency ν_{ml}) is

$$\gamma_{ml}^{ji} = \frac{I_{ji}}{I_{ml}} = \frac{A_{ji} \kappa_{ji} h \nu_{ji}}{A_{ml} \kappa_{ml} h \nu_{ml}} \frac{B_j}{B_m} \left[\frac{N_j}{N_m} \right]_{\rm eq} , \tag{83}$$

where

$$\left[\frac{N_j}{N_m} \right]_{\rm eq} = \frac{g_j}{g_m} \exp\left[-\frac{E_j - E_m}{kT_e} \right] \tag{84}$$

is the density ratio in Boltzmann equilibrium.

The intensity of radiation produced by dielectronic recombination to a terminating level i is

$$I_i^D = N_e N_+ \alpha_i^D \langle h \nu_{ai} \rangle \langle \kappa_{ai} \rangle \ , \tag{85}$$

where $\langle h \nu_{ai} \rangle$ is the average energy of the photons emitted in the $a \rightarrow i$ transitions and $\langle \kappa_{ai} \rangle$ is the effective escape factor for these transitions. Thus the total intensity of radiation produced in the plasma by all the dielectronic recombinations can be given as

$$I_{\rm di} = \sum_{i=1}^{3} I_i^D \ . \tag{86}$$

The autoionizing levels participating in populating of the terminating levels are spread out over a certain interval of energy. Therefore we calculate the average photon energy $\langle h \nu_{ai} \rangle$ as a weighted average,

$$\langle h \nu_{ai} \rangle = \sum_{a} g_a (E_a - E_i) \Big/ \sum_{a} g_a \ , \tag{87}$$

where E_a and g_a are energy and statistical weight, respectively, of the ath autoionizing level. The sums in Eq. (87) are taken over all the autoionizing levels available for recombination to the ith terminating level.

The continuum spectrum of the free-bound radiation is specified in terms of the net power radiated per unit plasma volume, per unit solid angle, and per unit frequency range. The free-bound monochromatic emission coefficient[48] $j_\nu^{\rm fb}$, in W cm^{-3} sr^{-1} s is

$$j_\nu^{\rm fb}(\nu) = 10^{-7} \sum_{i}^{\infty} \frac{h(2\nu a_0)^3}{c^2} \left[\frac{\pi \mathcal{R}}{kT_e} \right]^{3/2} \sigma_{ic}(\nu) \kappa_{ci} \frac{g_i}{g_+} \times N_e N_+ \exp\left[-\frac{h\nu - (U_i - \Delta E_\infty)}{kT_e} \right] , \tag{88}$$

if the assumption of Maxwellian distribution for electrons is valid. The possible shift (lowering) of the ionization energies in a high-density plasma can be estimated assuming that ions are much less mobile than the electrons and can be treated as point charges. Then, the reduction of the ionization potential is[44,48]

$$\Delta E_\infty = \frac{ze^2}{\rho_D} \ , \tag{89}$$

where

$$\rho_D = \left[\frac{kT_e}{4\pi e^2 (N_e + N_+)} \right]^{1/2} . \tag{90}$$

The coefficient for free-free emission (bremsstrahlung) caused by the acceleration of electrons in the field of nonhydrogenic ions, with the assumption of Maxwellian electron distribution, is given by[48]

$$j_\nu^{\rm ff}(\nu) = \frac{5.44 \times 10^{-46} G_{\rm ff}(\nu, T_e) z^2 N_e N_+ \exp(-h\nu/kT_e)}{T_e^{1/2}} \times [1 + D(\nu, T_e)] \tag{91}$$

in W cm^{-3} sr^{-1} s. In the emission frequency and electron temperature ranges consider in this work, the Gaunt factor $G_{\rm ff}$ is close to unity.[69] The correction factor $D(\nu, T_e)$ for the nonhydrogenic effects, evaluated by Asinovskii, Kirillin, and Kobsev,[70] is

$$D(\nu, T_e) = -0.084 - 0.0182(1.3 - T_e) - 0.145 \sin(0.6898\nu) \ , \tag{92}$$

where T_e and ν are given in units of 10^4 K and 10^4 cm^{-1}, respectively.

The total power emitted in all directions per unit volume for the free-bound and free-free continuum radiation can be obtained by multiplying Eqs. (88) and (91) by $4\pi\, d\nu$ and integrating over all possible frequencies ν. The integral does not exist in close form in case of the free-bound intensity. However, this intensity for the $c \rightarrow i$ transition can be calculated as

$$I_{ci} = N_e N_+ \alpha_{ci}^R \kappa_{ci} \langle \varepsilon_i \rangle \ , \tag{93}$$

where the average photon energy $\langle \varepsilon_i \rangle$ is taken as equal to $U_i + 3kT_e/2$. One should add that the total free-bound intensity ($I_{\rm fb} = \sum_i I_{ci}$) calculated by using the expression (93) agrees within several percent with the nu-

merically integrated value.

The total intensity of the bremsstrahlung emission (neglecting the reverse bremsstrahlung) is[48]

$$I_{\rm ff}=1.426\times10^{-34}\langle G_{\rm ff}(\nu,T_e)\rangle z^2 N_e N_+ T_e^{1/2} \times[1+\langle D(\nu,T_e)\rangle] \quad (94)$$

in W cm^{-3} where the averaged Gaunt factor $\langle G_{\rm ff}(\nu,T_e)\rangle$ and the average nonhydrogenic correction factor $\langle D(\nu,T_e)\rangle$ are close, in the temperature range considered in this work, to 1.2 and -0.15, respectively. The total intensity of the plasma radiation is calculated as

$$I_{\rm tot}=I_{\rm bb}+I_{\rm di}+I_{\rm fb}+I_{\rm ff} . \quad (95)$$

XI. RELAXATION TIMES

If population of an atomic level departs (as a result of a small change of plasma parameters) from its steady-state value, then some time τ (called the relaxation time) is needed to reestablish the steady-state population of the level.

Rearranging the terms populating and depopulating the ith level [Eq. (2)] one obtains[68,71]

$$\frac{\partial N_i}{\partial t}=-N_i\left[\sum_{k\,(<i)}(N_e R_{ik}+A_{ik})+\sum_{j\,(>i)}\left[N_e C_{ij}+\frac{N_j}{N_i}(1-\kappa_{ji})A_{ji}\right] +N_e S_{ic}+\frac{N_e N_+}{N_i}[(1-\kappa_{ci})\alpha_{ci}^R+(1-\langle\kappa_{ai}\rangle)\alpha_i^D]\right] + \sum_{k\,(<i)}N_k\left[N_e C_{ki}+\frac{N_i}{N_k}(1-\kappa_{ik})A_{ik}\right]+\sum_{j\,(>i)}N_j(N_e R_{ji}+A_{ji})+N_e N_+(\alpha_{ci}^R+\alpha_i^D+N_e\beta_{ci}) , \quad (96)$$

and the relaxation time for the ith level

$$\tau_i=\left[\sum_{k\,(<i)}(N_e R_{ki}+A_{ki})+\sum_{j\,(>i)}\left[N_e C_{ij}+\frac{N_j}{N_i}(1-\kappa_{ji})A_{ji}\right]+N_e S_{ic}+\frac{N_e N_+}{N_i}[(1-\kappa_{ci})\alpha_{ci}^R+(1-\langle\kappa_{ai}\rangle)\alpha_i^D]\right]^{-1} . \quad (97)$$

The expression (97), when used for the ground state (neglecting the deexcitation terms), gives rather the time for complete ionization of the ground state than the relaxation time defined above. However, this "ionization" time can be used as a crude measure of order of magnitude of the relaxation time for the ground state.

The relaxation times obtained in this work are given in Table VII. These times were calculated without taking into account the transient coupling between levels. Therefore they should be treated as estimates of order of magnitude of real relaxation times. One should also remember that any comparison of experimental data characterizing collisional-radiative nonequilibrium with results of theoretical steady-state calculations must be made with a great deal of caution. Steady-state models often assume that the populations of all levels, including the ground state, are time independent. Experimental plasmas are not quiescent but rather in transient conditions. Usually, the transients are much longer than the relaxation times for the excited electronic levels, but they are often much shorter than the relaxation times for the atomic ground state (see Table VII and Refs. 68, 71, and 72). In such cases the assumption of the quasisteady state (when all levels, with the exception of the ground state, do not suffer a temporal change in population density) can be used to obtain the time rate of change for population of the ground state.[13] If the experimental transient times for the excited levels are shorter than the levels relaxation times then the transient solution of the rate equations must be obtained (see, for example, Refs. 72 and 73, and references within).

XII. RESULTS AND DISCUSSION

The results of this work are presented as a function of the electron temperature T_e and the particle density N_t.

TABLE VII. Relaxation times (in seconds) for the $i=1,2,4,5$ levels of atomic nitrogen.

T_e (K)	N_e (cm^{-3})	$i=1$	$i=2$	$i=4$	$i=5$
8000	10^{10}	3.6×10^{-1}	2.6×10^{-2}	2.4×10^{-9}	2.1×10^{-9}
	10^{13}	3.5×10^{-4}	2.6×10^{-5}	2.3×10^{-9}	2.0×10^{-9}
	10^{16}	3.6×10^{-7}	2.6×10^{-8}	3.9×10^{-11}	4.2×10^{-11}
10000	10^{10}	1.4×10^{-1}	2.0×10^{-2}	2.4×10^{-9}	2.1×10^{-9}
	10^{13}	1.3×10^{-4}	2.0×10^{-5}	2.3×10^{-9}	2.0×10^{-9}
	10^{16}	1.4×10^{-7}	2.0×10^{-8}	3.4×10^{-11}	3.9×10^{-11}
13000	10^{10}	6.0×10^{-2}	1.5×10^{-2}	2.4×10^{-9}	2.1×10^{-9}
	10^{13}	6.0×10^{-5}	1.5×10^{-5}	2.2×10^{-9}	2.0×10^{-9}
	10^{16}	6.0×10^{-8}	1.5×10^{-8}	3.0×10^{-11}	3.7×10^{-11}

The density N_t is the total density of charged particles (bound and free) considered in the model, i.e.,

$$N_t = 2N_a + N_+ + N_e \ , \tag{98}$$

where $N_a = \sum_i N_i$ is the total atomic density. We assume in our calculations that the free ions are singly ionized. This and the assumption that the plasma is electrically neutral imply that the total density of the free charged particles is $N_+ + N_e$, while the total density of the charged particles bound in atomic species is equal to $2N_a$ [one electron and one ion (the atomic core)]. It should be emphasized that T_e and N_t are the natural constants of the steady-state plasma with no applied fields. Each set of these two constants *uniquely* specifies the nonequilibrium properties of the stationary plasma; all the other properties, including N_e, depend on T_e and N_t. The common procedure, presenting the properties of plasma as function of T_e and N_e, is often inappropriate because it forces a strong nonequilibrium; in particular, the plasma may not be able to produce the assumed N_e at a given T_e. Therefore the appropriate and practically useful way of presenting nonequilibrium properties of stationary plasmas is to show these properties as functions of the particle density N_t (representing the conservation of particles in the plasma) and electron temperature T_e (representing the thermal energy of electrons), with the assumption of plasma charge neutrality (one should remember that in partially ionized plasmas $N_t \approx 2N_a$).

The range of plasma density and temperature chosen in our calculations is limited by the following assumptions: (i) the atom-atom inelastic collisions do not contribute to the properties of the plasma, and (ii) the role of doubly ionized ions and excited singly ionized ions is negligible. The first assumption requires that $T_e \gtrsim 8000$ K (at higher densities),[10,11] while the second is justified if $N_e/N_a \ll 1$ (see Ref. 1). Therefore some of the high-temperature results (those for which the later requirement is not closely followed) presented in some figures should be treated as crude estimates.

Numerical calculations show that the densities of the atoms excited to the $i=2$ and 3 levels are in Boltzmann equilibrium with the ground state in the entire range of conditions considered here (Fig. 7). In addition, the populations of atoms excited to these two levels are close to the population of the ground-state atoms. This is mainly due to the lack of radiative coupling of these levels with the ground state and the relatively small energy gaps between the levels (Fig. 1). The fact that the fraction of atoms excited to the $i=2$ and 3 levels is large, is important for the redistribution of energy in the plasma and for the plasma transport properties (the electric and thermal conductivity, electron mobility, etc.). These properties depend on the electron-atom cross sections for elastic scattering, which are greater for electron scattering by excited atoms than for scattering by the ground-state atoms.

The populations of several upper levels are given, as ratios B_i [Eq. (7)], in Fig. 8. The populations show almost linear N_t dependence at low densities. At higher densities, the frequencies of collisions producing the upper levels and the reabsorption of radiation increase. Then, the populations of the upper levels reach Boltzmann equilibrium ($B_i = 1$).

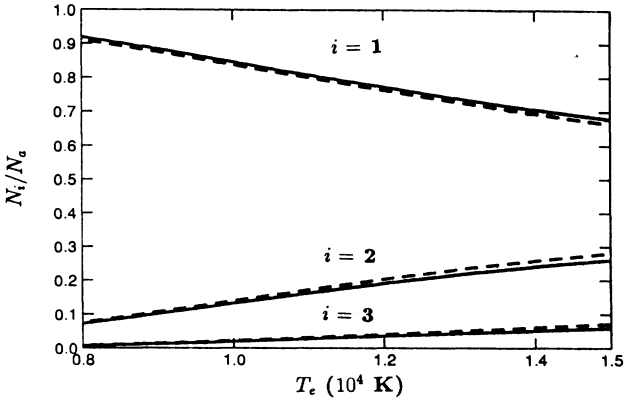

FIG. 7. Densities N_i of nitrogen atoms in the ground state ($i=1$), in the first excited ($i=2$), and in the second excited ($i=3$) levels. N_a is the atomic density and T_e is the electron temperature. The total particle densities N_t are 10^{13} cm^{-3} (solid lines) and 10^{18} cm^{-3} (dashed lines).

It is convenient to introduce a ratio

$$\rho_i = \frac{N_i}{N_i^S} = \frac{B_i}{H_{n_{\max}}} \ , \tag{99}$$

where N_i^S is the Saha population of the level i. (This ratio is a measure of the departure of the ith level population from Saha equilibrium.) The ratios ρ_i for several levels and several temperatures are shown in Fig. 9. As expected, the lowest three levels are far from Saha equilibrium, for all temperatures, at low and medium densities since these levels are far from continuum and their populations are totally controlled by the collisions involving the levels. The upper levels ($i \geq 4$) are close to each other and to continuum. Therefore their departure from Saha equilibrium is always smaller than that of the levels $i=1$, 2, and

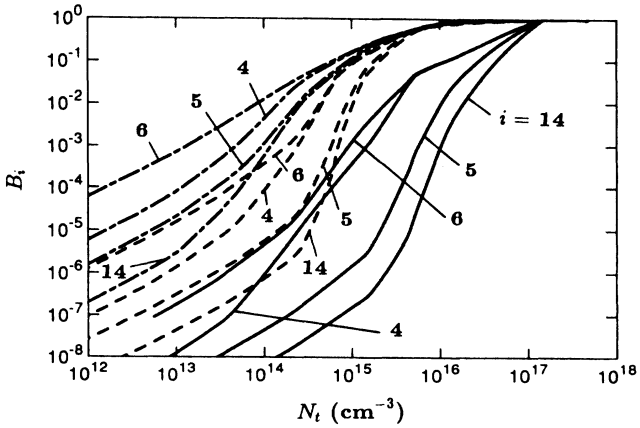

FIG. 8. Population (coefficients B_i) of nitrogen atoms excited to the $i=4$, 5, 6, and 14 levels. N_t is the total particle density. The electron temperatures are 8000 (solid lines), 10 000 (dashed lines), and 13 000 K (dot-dashed lines).

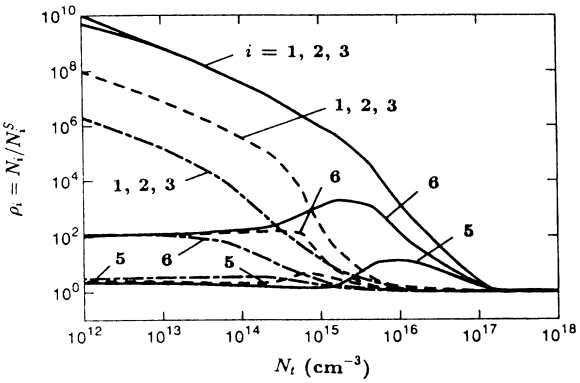

FIG. 9. Population (coefficients ρ_i) of nitrogen atoms excited to $i=1$, 2, 3, 5, and 6 levels. N_t is the total particle density. The electron temperatures are 8000 (solid lines), 10 000 (dashed line), and 13 000 K (dot-dashed lines).

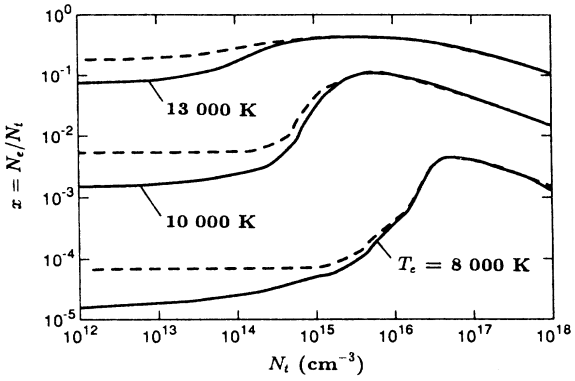

FIG. 11. Ionization degree $x=N_e/N_t$ (solid lines) of the atomic nitrogen plasma as a function of the particle density N_t and electron temperature T_e. The dashed lines give the ionization degree when dielectronic recombination is neglected.

3. As the plasma density increases, the departure of the upper levels from Saha equilibrium reaches maximum (at $10^{15}-10^{16}$ cm^{-3}) corresponding to the maximum ionization degree of the plasma (see Fig. 11). This is because the reabsorption of the dipole-allowed radiation, increasing with density, improves conditions for Boltzmann equilibrium. Further increase of the density causes only a small increase in reabsorption of the radiation but a substantial increase in electron density. Then, all the levels are in collisional Saha equilibrium with electrons.

The production of electrons in atomic nitrogen is shown, as function of T_e and N_t, in Figs. 10 and 11. One can see that the population of electrons is quite high (in other words, it is quite easy to ionize atomic nitrogen) in the entire range of T_e and N_t considered. This is due to the fact that the lowest, highly populated metastable atomic levels contribute significantly to the ionization of the gas. The ionization degree ($x=N_e/N_t$) increases significantly when N_t approaches values of $10^{15}-10^{16}$ cm^{-3} because at these densities the overall efficiency of the electron-impact upward processes and reabsorption of the dipole-allowed radiation reaches its maximum. At higher N_t, the electrons reach Saha equilibrium. As can be seen from Figs. 10 and 11 the dielectronic recombination is important for the production of electrons at lower densities ($N_t \lesssim 10^{15}$ cm^{-3}) in the entire range of temperatures considered.

The plasma radiation escape factors were calculated by assuming plasma thickness $L=4$ cm and atomic temperature $T_a=T_e$ (an accurate value of the atomic temperature is not of significant importance because the Doppler width [Eq. (66)] is not a strong function of T_a). The escape factors κ_{ji} for several electric dipole-allowed transitions are given in Figs. 12 and 13 as functions of N_t and T_e. At low density the plasma is transparent ($\kappa_{ji}\approx 1$) to the radiation. At higher N_t, the dipole-allowed lines are absorbed efficiently due to the high density of the absorbing atoms (those with $i\leq 3$) (then the escape factors κ_{ji} approach the Holstein[12] limit [Eq. (73)]). The reabsorption of the electric dipole-forbidden radiation is weak over the entire range of conditions considered here because of the very small values of the oscillator strengths for the transitions.

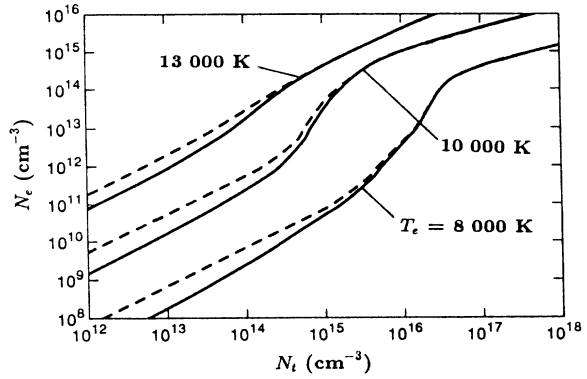

FIG. 10. Production of electrons (solid lines) in the atomic nitrogen plasma as a function of the particle density N_t and electron temperature T_e. The dashed lines give the electron density when dielectronic recombination is neglected.

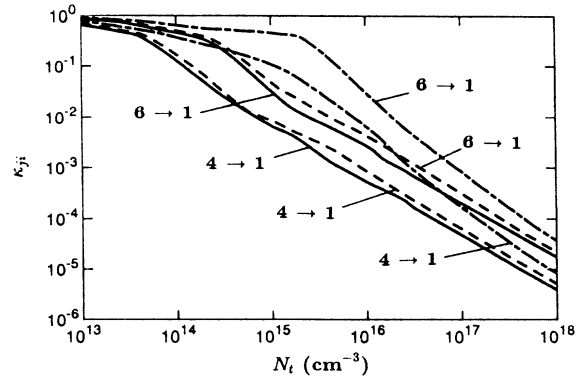

FIG. 12. N_t dependence of the radiation escape factors κ_{ji} for the 4→1 and 6→1 electric dipole-allowed lines in the atomic nitrogen plasma. The electron temperatures are 8000 (solid lines), 10 000 (dashed lines), and 13 000 K (dot-dashed lines).

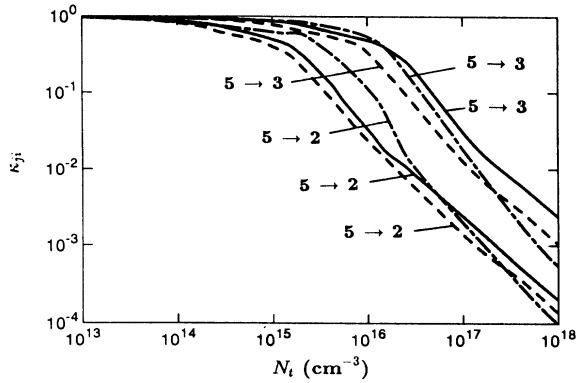

FIG. 13. N_t dependence of the radiation escape factors κ_{ji} for the 5→2 and 5→3 electric dipole-allowed lines in the atomic nitrogen plasma. The electron temperatures are 8000 (solid lines), 10 000 (dashed lines), and 13 000 K (dot-dashed lines).

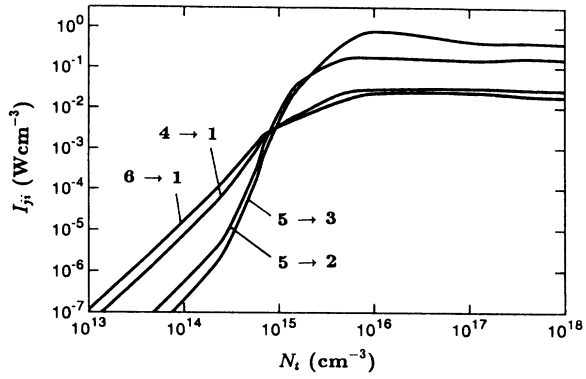

FIG. 15. N_t dependence of the line intensities I_{ji} for the 4→1, 6→1, 5→2, and 5→3 electric dipole-allowed transitions in the atomic nitrogen plasma. The electron temperature is 10 000 K.

The intensities of several electric dipole-allowed lines are shown in Figs. 14–16. As expected, these intensities increase with T_e due to simultaneous increase in production of the upper radiative levels which results from the increase of frequency of collisional excitation. At low and medium densities ($N_t \lesssim 10^{15}$ cm^{-3}), the line intensities are proportional to the plasma density. At higher densities the atomic levels are in Boltzmann equilibrium and plasma electrons are in Saha equilibrium. Then, the net production of the dipole-allowed radiation is density independent.

Various kinds of radiation produced in the atomic nitrogen plasma are discussed in Figs. 17–19. At low and medium densities bound-bound radiation dominates the plasma radiation, whereas the much smaller total intensities of the free-bound and dielectronic radiation are competing with each other within an order of magnitude. At higher densities, the free-bound and free-free radiation is becoming important and at $T_e > 10\,000$ K the latter radiation is dominant. This is caused by the fact that at these densities the reabsorption of the dipole-allowed radiation

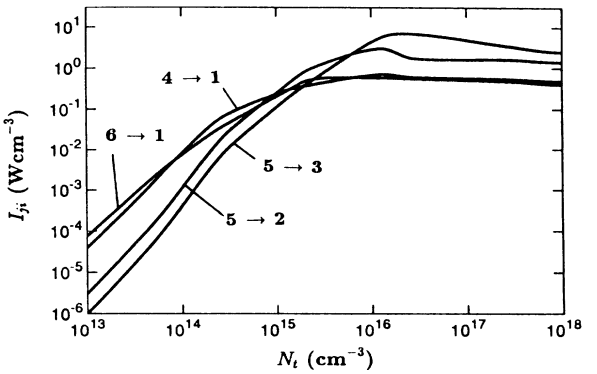

FIG. 16. N_t dependence of the line intensities I_{ji} for the 4→1, 6→1, 5→2, and 5→3 electric dipole-allowed transitions in the atomic nitrogen plasma. The electron temperature is 13 000 K.

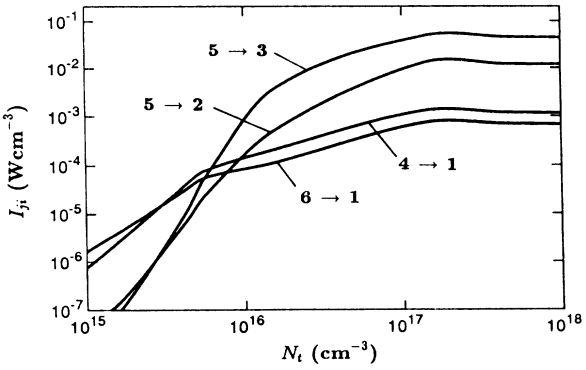

FIG. 14. N_t dependence of the line intensities I_{ji} for the 4→1, 6→1, 5→2, and 5→3 electric dipole-allowed transitions in the atomic nitrogen plasma. The electron temperature is 8000 K.

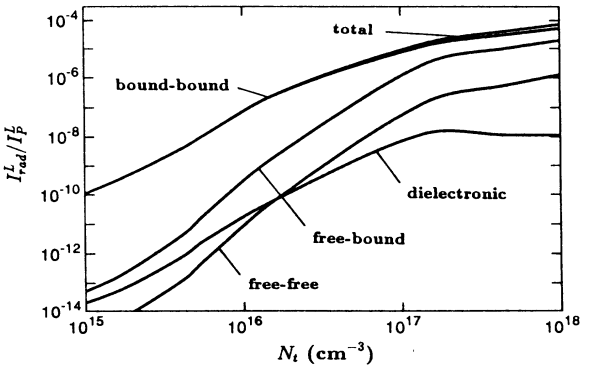

FIG. 17. N_t dependence of the ratios of the bound-bound (I^L_{bb}), dielectronic (I^L_{di}), free-bound (I^L_{fb}), free-free (I^L_{ff}), and the total radiation intensity (I^L_{tot}) to the Planck (blackbody) intensity (I^L_P) in the atomic nitrogen plasma. $I^L_{rad} = I_{rad} L/4\pi$ and $L = 4$ cm. The electron temperature is 8000 K.

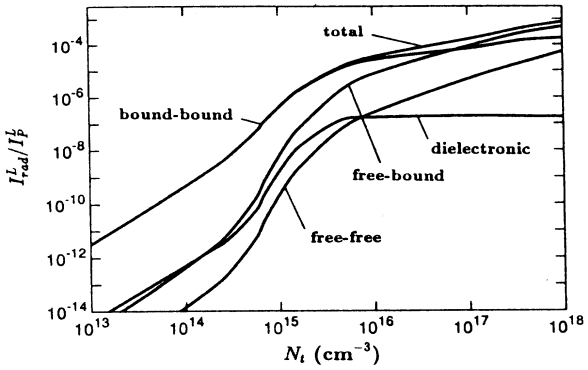

FIG. 18. N_t dependence of the ratios of the bound-bound (I^L_{bb}), dielectronic (I^L_{di}), free-bound (I^L_{fb}), free-free (I^L_{ff}), and the total radiation intensity (I^L_{tot}) to the Planck (blackbody) intensity (I^L_P) in the atomic nitrogen plasma. The electron temperature is 10 000 K.

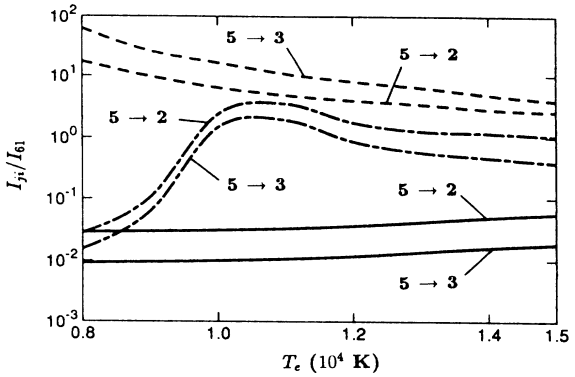

FIG. 20. T_e dependence of the line intensity ratios γ^{ji}_{61} of the dipole-allowed 5→2 and 5→3 transitions to the dipole-allowed 6→1 transition in the atomic nitrogen plasma with $N_t = 10^{13}$ (solid lines), 10^{15} (dot-dashed lines), and 10^{18} cm^{-3} (dashed lines).

is much stronger than the reabsorption of the free-bound and free-free radiation. Dielectronic radiation, competing at low densities with the free-bound radiation, is strongly reabsorbed at higher densities and its relative importance becomes negligible. Finally, one should note that the total plasma radiation emission is far from the blackbody emission even at higher densities.

Temperature-dependent intensity ratios of several dipole-allowed lines are given in Fig. 20. Some of them can be useful for plasma diagnostics (when the ratios are strong functions of T_e; see discussion in Ref. 74, but in a rather limited range of the electron temperature. In situations when the weak emission of some of the forbidden lines is detectable, the ratios of the forbidden line intensities to the allowed line intensities can be quite suitable for the plasma diagnostics. An example of a particularly useful choice of such ratios is given in Fig. 21.

Relaxation times for various atomic levels are given in Table VII. Lack of radiative transitions from the two lowest excited levels to the ground state causes the relaxation times for the ground atomic state to be unusually short (for example, the corresponding times for atomic hydrogen plasma are much longer[68]). Thus (a) the assumption of the quasisteady state in atomic nitrogen plasmas is quite realistic, and (b) the assumption of steady state in the plasmas can often be extended to the atomic ground state.

Experimental work on kinetics of high-temperature nitrogen is very limited; the only existing data are frequency-dependent measurements of continuum (free-free plus free-bound) radiation produced in high-density nitrogen behind gas-dynamic shocks[75] and in arc discharges.[70,76,77] A comparison of these measurements and our calculations for the total emission coefficient $j_\nu = j^{fb}_\nu + j^{ff}_\nu$ is given in Fig. 22. (The typical "sawtooth" form appearing in the theoretical predictions is due to the merging of the continuum lines.[78]) The calculations in-

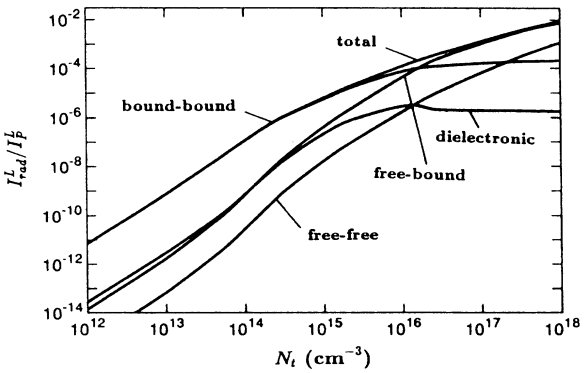

FIG. 19. N_t dependence of the ratios of the bound-bound (I^L_{bb}), dielectronic (I^L_{di}), free-bound (I^L_{fb}), free-free (I^L_{ff}), and the total radiation intensity (I^L_{tot}) to the Planck (blackbody) intensity (I^L_P) in the atomic nitrogen plasma. The electron temperature is 13 000 K.

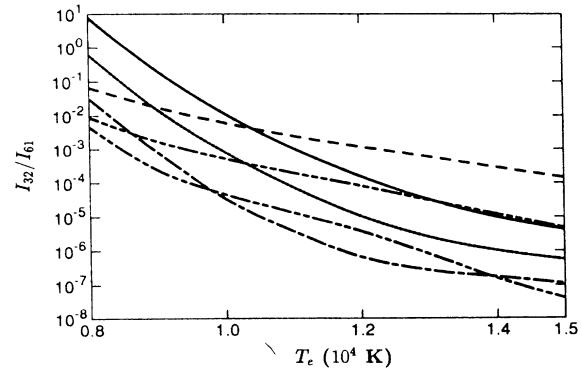

FIG. 21. T_e dependence of the line intensity ratio γ^{32}_{61} of the dipole-forbidden 3→2 transition to the dipole-allowed 6→1 transition in the atomic nitrogen plasma with $N_t = 10^{13}$ (solid line), $N_t = 10^{14}$ (dotted line), 10^{15} (dot-dashed line), 10^{16} (double-dot–dashed line), 10^{17} (triple-dot–dashed line), and 10^{18} cm^{-3} (dashed line).

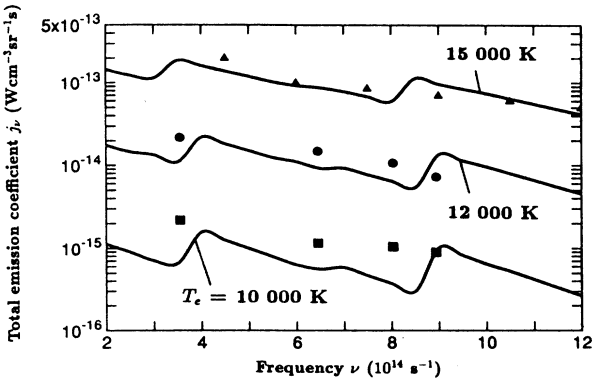

FIG. 22. Comparison of the calculated (solid lines) and measured total continuum emission coefficients $j_\nu = j_\nu^{fb} + j_\nu^{ff}$ for $T_e = 10000$ K, $P = 0.61$ atm (Ref. 75, squares), $T_e = 12000$ K, $P = 0.78$ atm (Ref. 75, circles), and $T_e = 15000$ K, $P = 1$ atm (Ref. 70, triangles).

clude the free-bound and free-free radiation with the electron density N_e obtained from the solution of the 14-level collisional-radiative model (as discussed above, this number of the atomic levels leads to a reliable prediction of plasma properties, including the electron density). Since part of the measured continuum spectrum is in the low-frequency region we calculated the total free-bound emission as a sum of radiation produced in the free-bound transitions to 24 atomic levels; the highly excited ($14 < i \leq 24$) levels are in Saha equilibrium with electrons under the experimental conditions. The hydrogenic photoionization cross section,[48]

$$\sigma_{ic}^{H}(\nu) = \pi a_0^2 \frac{64\alpha}{3^{3/2}} \left[\frac{\mathcal{R}}{h\nu} \right]^{3/2} \frac{z^4}{n^5} G_i(n,u) , \tag{100}$$

and the cross section (53) are used in calculations of the intensity of the free-bound emission to the highly excited ($14 < i \leq 24$) levels. Here n is the principal quantum number for the excited level and the Gaunt factor G_i can be approximated by[51]

$$G_i(n,u) = 1 + 0.1728 n^{-2/3}(u+1)^{-2/3}(u-1) - 0.0496 n^{-4/3}(u+1)^{-4/3}(u^2 + \tfrac{4}{3}u + 1) \tag{101}$$

and

$$u = n^2 \varepsilon' , \tag{102}$$

with ε' in rydbergs and α being the fine-structure constant. The hydrogenic cross section (100) can be used for determination of the free-bound radiation resulting from the transitions to the levels with $i > 14$ because the quantum defects for the transitions are close to zero. Then, the nonhydrogenic photoionization cross section (54) converges to the hydrogenic cross section (100).

The continuum radiation is dominated in the low-frequency part of the spectrum in Fig. 22 by bremsstrahlung. In the higher-frequency region ($4 \times 10^{14} \lesssim \nu \lesssim 1.2 \times 10^{15}$ s^{-1}), the free-bound radiation [mainly to the intermediate ($3 < i \leq 14$) levels] dominates the production of the continuum radiation. The agreement of the measured continuum emission coefficient with the present calculations is good over the temperature range from 10 000 to 15 000 K. (One should note that a difference of a factor of 2 in the emission coefficient means only 40% difference in the electron density because the coefficient is proportional to N_e^2 in electrically neutral plasmas.) The calculated total continuum emission coefficient differs slightly from the measured values only at lower T_e (10 000 K). The uncertainty of T_e for the shock tube measurements was several hundred degrees, which could mean a noticeable uncertainty in determination of N_e. The uncertainty in T_e would have greater effect on the low-temperatures measurements than on the higher-temperature measurements because the frequency of inelastic collisions (important for production of electrons) changes more rapidly at the lower values of T_e. A part of the difference between the measured and calculated values of the coefficient j_ν at lower temperatures could also result from the fact that the atomic ground states in the experimental plasmas were in transient states (i.e., the plasmas were in a quasisteady state, as discussed above in conjunction with the relaxation times). In a quasisteady state $dN_a/dt = -dN_e/dt$, so that the experimental electron density might have been different than the value used in the calculations and this difference would be more visible at lower temperatures (see Table VII). However, this effect should not have been large due to the high electron density in the discussed experiments.

It was hypothesized[70,75-77] that the excess of radiation might have been caused by photon emission associated with production of negative ions N^- by radiative attachment. However, some recent work[79,80] has clearly indicated that the ground-state (^3P) N^- ion is not stable. One can see that inclusion of the N^- negative ion continuum emission in collisional-radiative models of atomic nitrogen is neither appropriate nor needed for correct interpretation of the mechanisms producing the plasma continuum radiation. This conclusion is also in agreement with the conclusion of Cooper,[81] who did not observe negative ion continuum radiation in his experiments.

The accuracy of the final results of this work depends on the accuracies of the cross sections and Einstein coefficients used in the rate equations (in general, the latter are far more accurate than the former). As discussed above, experimental data on almost all the considered cross sections are not available in literature. Therefore one has to use the theoretical predictions of accuracy that cannot be verified by a direct comparison with experiment. However, some conclusions can be drawn from a comparison of the theoretical cross sections for various atomic systems with the available measurements. The comparison suggests that the accuracy of the theoretical cross sections should be better, in most cases (with possible exception of transitions between highly excited levels), than a factor of 2. More accurate quantum-mechanical methods such as close-coupling and R-matrix methods are available (see the cooperative opacity program of Seaton[82]). These calculations include strong coupling effects, electron correlation effects, and polarization

effects, but they are very computer and people time intensive and have been completed for only a few systems. Therefore, using approximate methods, such as, for example, the Vainshtein approach, is practically necessary in the modeling of collisional-radiative nonequilibrium in most gases, including atomic nitrogen. It should also be added that reasonable inaccuracies in the cross sections for transitions in these gases often do not lead to significant quantitative inaccuracies and/or qualitative differences in the nonequilibrium properties. This can be seen in the widely studied case of collisional-radiative nonequilibrium in atomic hydrogen. Even though different sets of cross sections were used in almost each study, in many cases (including plasmas with different optical thickness) the differences in overall nonequilibrium properties of hydrogen were not large. However, in order to establish a detailed dependence between the reliability of the collisional-radiative models and the accuracy of the cross sections used in the models one should use the sets of cross sections obtained either from experiment or from the complex and time-consuming calculations such as the cooperative opacity program.

In summary, it seems that the present model gives acceptable predictions for nonequilibrium populations of electrons and excited atoms, as well as the production of radiation in partially ionized atomic nitrogen. One should keep in mind, however, the remarks given above and the fact that the radiation escape factors of this work are based on the two-level model, which neglects the multilevel coupling effects.

ACKNOWLEDGMENTS

The authors thank Alex Dalgarno, Verne Jacobs, Gillian Peach, and Simon Suckewer for their comments. This work was supported by the National Aeronautics and Space Administration, Grant No. NAGW-1061 and the U.S. Air Force Office of Scientific Research, Grants No. 88-0119 and No. 88-0146.

[1]R. D. Taylor and A. W. Ali, J. Quantum Spectrosc. Radiat. Transfer **35**, 213 (1986).
[2]E. J. Stone and E. C. Zipf, Phys. Rev. A **4**, 610 (1971).
[3]E. J. Stone and E. C. Zipf, J. Chem. Phys. **58**, 4278 (1973).
[4]J. Bacri, M. Lagreca, and A. Medani, Physica B+C **113C**, 403 (1982).
[5]M. Kafatos and J. Lynch, Astrophys. J. Suppl. Ser. **42**, 611 (1980).
[6]J. L. Kulander, J. Quantum Spectrosc. Radiat. Transfer **5**, 253 (1965).
[7]C. Park, J. Quantum Spectrosc. Radiat. Transfer **8**, 1633 (1968).
[8]J. F. Shaw, M. Mitchner, and C. H. Kruger, Phys. Fluids **13**, 325 (1970).
[9]C. G. Braun and J. A. Kunc, Phys. Fluids **30**, 499 (1987).
[10]A. Skorupski and S. Suckewer, J. Phys. B **7**, 1401 (1974).
[11]J. A. Kunc, Phys. Fluids **30**, 2255 (1987).
[12]T. Holstein, Phys. Rev. **83**, 1159 (1951).
[13]D. R. Bates, A. E. Kingston, and R. W. P. McWhirter, Proc. R. Soc. London Ser. A **267**, 297 (1962).
[14]S. Suckewer, J. Phys. B **3**, 380 (1970).
[15]S. Suckewer, J. Phys. B **3**, 390 (1970).
[16]I. I. Sobelman, L. A. Vainshtein, and E. A. Yukov, *Excitation of Atoms and Broadening of Spectral Lines* (Springer-Verlag, New York, 1981).
[17]I. I. Sobelman and L. A. Vainshtein, J. Quantum Spectrosc. Radiat. Transfer **8**, 1491 (1968).
[18]R. J. W. Henry, P. G. Burke, and A. L. Sinfailam, Phys. Rev. **178**, 218 (1969).
[19]K. Smith, R. J. W. Henry, and P. G. Burke, Phys. Rev. **157**, 51 (1967).
[20]K. Smith, M. J. Conneely, and L. A. Morgan, Phys. Rev. **177**, 177 (1969).
[21]M. J. Seaton, in *The Airglow and the Aurorae,* edited by E. B. Armstrong and A. Dalgarno (Pergamon, London, 1956), p. 289.
[22]L. Vriens, Phys. Rev. A **141**, 88 (1966).
[23]P. Mansbach and J. Keck, Phys. Rev. **181**, 275 (1969).
[24]E. Brook, M. F. A. Harrison, and A. C. H. Smith, J. Phys. B **11**, 3115 (1978).
[25]M. Gryzinski and J. A. Kunc, J. Phys. B **19**, 2479 (1986).
[26]J. A. Kunc, J. Phys. B **21**, 3619 (1988).
[27]R. H. Garstang, Proc. Cambridge Philos. Soc. **57**, 115 (1961).
[28]R. H. Garstang, Mon. Not. R. Astron. Soc. **111**, 115 (1951).
[29]C. Goldbach, M. Martin, G. Nollez, P. Plomdeur, J. P. Zimmermann, and D. Babic, Astron. Astrophys. **161**, 47 (1986).
[30]A. Hibbert, P. L. Dufton, and F. P. Keenan, Mon. Not. R. Astron. Soc. **213**, 721 (1985).
[31]H. Nussbaumer and P. J. Storey, Astron. Astrophys. Suppl. Ser. **56**, 293 (1984).
[32]M. W. Chang, Astrophys. J. **211**, 300 (1977).
[33]P. D. Dumont, E. Biemont, and N. Grevesse, J. Quantum Spectrosc. Radiat. Transfer **14**, 1127 (1974).
[34]A. K. Pradhan and H. E. Saraph, J. Phys. B **10**, 3365 (1977).
[35]C. J. Zeippen, M. J. Seaton, and D. C. Morton, Mon. Not. R. Astron. Soc. **181**, 527 (1977).
[36]D. B. Jenkins, J. Quantum Spectrosc. Radiat. Transfer **34**, 55 (1985).
[37]W. L. Wiese, M. W. Smith, and B. M. Glennon, *Atomic Transition Probabilities,* Natl. Bur. Stand. (U.S.), Natl. Stand. Ref. Data Ser. No. 4 (U.S. GPO, Washington, D.C., 1966), Vol. I.
[38]K. Butler and C. J. Zeippen, Astron. Astrophys. **141**, 274 (1984).
[39]T. Yamanouchi and H. Horie, J. Phys. Soc. Jpn. **7**, 52 (1952).
[40]H. Nussbaumer and P. J. Storey, Astron. Astrophys. **126**, 75 (1983).
[41]A. Burgess, Astrophys. J. **139**, 776 (1964).
[42]R. H. Bell and M. J. Seaton, J. Phys. B **18**, 1589 (1985).
[43]A. Burgess and H. P. Summers, Astrophys. J. **157**, 1007 (1969).
[44]J. C. Weisheit, J. Phys. B **8**, 5256 (1975).
[45]M. J. Seaton and P. J. Storey, in *Atomic Processes and Applications,* edited by P. G. Burke and B. L. Moiseiwitsch (North-Holland, Amsterdam, 1976), p. 135.
[46]V. L. Jacobs and J. Davis, Phys. Rev. A **18**, 697 (1978).
[47]V. L. Jacobs and M. Blaha, Phys. Rev. A **21**, 525 (1980).
[48]H. R. Griem, *Plasma Spectroscopy* (McGraw-Hill, New York, 1964).

[49]D. R. Bates, Case Stud. At. Phys. **4**, 57 (1974).
[50]E. A. Milne, Mon. Not. R. Astron. Soc. **81**, 361 (1921).
[51]D. R. Bates and A. Dalgarno, in *Atomic and Molecular Processes,* edited by D. R. Bates (Academic, New York, 1962), p. 245.
[52]A. Burgess and M. J. Seaton, Mon. Not. R. Astron. Soc. **120**, 121 (1960).
[53]G. Peach, Mem. R. Astron. Soc. **71**, 1 (1967).
[54]G. Peach, Mem. R. Astron. Soc. **71**, 13 (1967).
[55]G. Peach, Mem. R. Astron. Soc. **73**, 1 (1970).
[56]M. J. Seaton, Mon. Not. R. Astron. Soc. **118**, 504 (1958).
[57]R. J. Henry, Astrophys. J. **161**, 1153 (1970).
[58]M. J. Seaton, Rev. Mod. Phys. **30**, 979 (1958).
[59]A. Dalgarno, R. J. W. Henry, and A. L. Stewart, Planet. Space Sci. **12**, 235 (1964).
[60]A. Dalgarno and D. Parkinson, J. Atmos. Terr. Phys. **18**, 335 (1960).
[61]B. H. Armstrong, J. Quantum Spectrosc. Radiat. Transfer **7**, 61 (1967).
[62]S. Ganapathy and V. Parthasarathi, Indian J. Pure Appl. Phys. **15**, 63 (1977).
[63]D. G. Hummer, Mem. R. Astron. Soc. **70**, 1 (1965).
[64]D. W. Posener, Aust. J. Phys. **12**, 184 (1959).
[65]M. Otsuka, J. Quantum Spectrosc. Radiat. Transfer **21**, 489 (1979).
[66]M. Otsuka, R. Ikee, and K. Ishii, J. Quantum Spectrosc. Radiat. Transfer **21**, 41 (1979).
[67]E. H. Avrett and D. G. Hummer, Mon. Not. R. Astron. Soc. **130**, 295 (1965).
[68]H. W. Drawin, J. Quantum Spectrosc. Radiat. Transfer **10**, 33 (1970).
[69]G. B. Rybicki and A. P. Lightman, *Radiative Processes in Astrophysics* (Wiley, New York, 1979).
[70]Z. J. Asinovskii, A. V. Kirillin, and G. A. Kobsev, J. Quantum Spectrosc. Radiat. Transfer **10**, 143 (1970).
[71]R. W. P. McWhirter and A. G. Hearn, Proc. Phys. Soc. **82**, 641 (1963).
[72]M. Cacciatorie, M. Capitelli, and H. W. Drawin, Physica B+C **84C**, 267 (1976).
[73]C. C. Limbaugh and A. A. Mason, Phys. Rev. A **4**, 2368 (1971).
[74]J. A. Kunc, J. Appl. Phys. **63**, 656 (1988).
[75]D. L. Ciffone and J. G. Borucki, J. Quantum Spectrosc. Radiat. Transfer **11**, 1291 (1971).
[76]G. M. Thomas and W. A. Menard, AIAA J. **5**, 2214 (1967).
[77]G. Boldt, Z. Phys. **154**, 330 (1959).
[78]B. H. Armstrong, J. Quantum Spectrosc. Radiat. Transfer **4**, 207 (1964).
[79]H. S. W. Massey, *Negative Ions* (Cambridge University Press, Cambridge, England, 1976).
[80]H. S. W. Massey, in *Advances in Atomic and Molecular Physics,* edited by D. R. Bates and B. Bederson (Academic, New York, 1979), p. 1.
[81]D. M. Cooper, J. Quantum Spectrosc. Radiat. Transfer **12**, 1175 (1972).
[82]A. K. Pradhan, in *Atomic Processes in Plasmas,* edited by A. Hauer and A. L. Mertf (Academic, New York, 1988), p. 1 (and references within).
[83]S. M. V. Aldrovandi and D. Pequignot, Astron. Astrophys. **25**, 137 (1973).
[84]J. M. Shull and M. van Steenberg, Astrophys. J. **48**, 95 (1982).